BOREAS An international journal of Quaternary research

Palaeolimnological conditions inferred from fossil diatom assemblages and derivative spectral properties of sediments in thermokarst ponds of subarctic Quebec, Canada

FRÉDÉRIC BOUCHARD, REINHARD PIENITZ, JOSEPH D. ORTIZ, PIERRE FRANCUS AND ISABELLE LAURION

BOREAS

Bouchard, F., Pienitz, R., Ortiz, J. D., Francus, P. & Laurion, I. 2013 (July): Palaeolimnological conditions inferred from fossil diatom assemblages and derivative spectral properties of sediments in thermokarst ponds of subarctic Quebec, Canada. *Boreas*, Vol. 42, pp. 575–595. 10.1111/bor.12000. ISSN 0300-9483.

Thermokarst ponds are widespread in arctic and subarctic regions, but little is known about their temporal evolution prior to human observations. This paper presents a pioneer biostratigraphic study conducted at a subarctic site with limnologically contrasted ponds located on the eastern shore of Hudson Bay, Canada. Fossil diatom and visible near infrared (VNIR) derivative spectral analyses were performed on short sediment cores, confirming the occurrence of three distinct stratigraphic facies as already inferred from an anterior sedimentological study: a lacustrine upper facies (UF) and a marine lower facies (LF), separated by an organic-rich/peat transitional zone (TZ). Diatoms were almost absent from LF, but increased significantly in both TZ and UF. Identified diatom taxa were mainly benthic species (e.g. genera *Fragilaria*, *Pinnularia*), and their down-core distribution appeared to be related to dissolved organic carbon (DOC) and possibly pH conditions. Diatom-inferred DOC showed a decreasing trend towards the surface (potentially associated with an increase in pH), inverse to the general trend in this region, suggesting the action of other mechanisms on DOC, such as exhaustion of external inputs from limited catchments and the role of discontinuous peat layers (former surfaces of permafrost mounds) during the initial stages of pond formation. These bryophilous substrates in aerophilic habitats probably controlled diatom community composition. The combination of diatom and VNIR data revealed similar trends between (i) opal (amorphous silica) and diatom abundances; (ii) eukaryotic/prokaryotic algae ratio and anoxia or hypoxia in bottom waters; and (iii) limonite (iron oxide) and redox conditions in surface sediments. These findings indicate that diatom community changes and pond limnological evolution in the recent past were controlled mainly by autogenic processes (e.g. local vegetation/soil development, peat accumulation and erosion), rather than by allogenic forcing mechanisms (e.g. precipitation and temperature, geochemical leaching of the surrounding glaciomarine sediments).

Frédéric Bouchard (frederic.bouchard@cen.ulaval.ca), Pierre Francus (pierre.francus@ete.inrs.ca) and Isabelle Laurion (isabelle.laurion@ete.inrs.ca), Institut national de la recherche scientifique, Centre Eau Terre Environnement (INRS-ETE), 490 de la Couronne, Québec, QC, Canada G1K 9A9, and Centre d'études nordiques (CEN), Pavillon Abitibi-Price, 2405 de la Terrasse, Université Laval, Québec, QC, Canada G1V 0A6; Reinhard Pienitz (reinhard.pienitz@cen.ulaval.ca), Département de Géographie, Pavillon Abitibi-Price, 2405 de la Terrasse, Université Laval, Québec, QC, Canada G1V 0A6, and Centre d'études nordiques (CEN), Pavillon Abitibi-Price, 2405 de la Terrasse, Université Laval, Québec, QC, Canada G1V 0A6; Joseph D. Ortiz (jortiz@kent.edu), Department of Geology, Kent State University, Kent, OH 44242, USA; *received 30th January 2012, accepted 4th October 2012.*

Thermokarst ponds and lakes, formed by permafrost thawing and erosion at high latitudes, are becoming more widespread throughout the arctic and subarctic regions of northern Europe (Zuidhoff & Kolstrup 2000; Christensen *et al*. 2004), Siberia (Agafonov *et al*. 2004; Takakai *et al*. 2008), Alaska (Jorgenson *et al*. 2006; Osterkamp 2007) and Canada (Beilman *et al*. 2001; Payette *et al*. 2004; Vallée & Payette 2007). These aquatic ecosystems can persist from days to thousands of years, depending on regional climate and local factors such as substrate properties and hydrology (Pienitz *et al*. 2008). Vast amounts of organic carbon formerly trapped in permafrost and mobilized through global warming will be partly mineralized to CO_2 and CH_4 in aquatic systems, and then transferred to the atmosphere (Zimov *et al*. 2006; Schuur *et al*. 2009; Tarnocai *et al*. 2009). Thermokarst systems can thus act as biogeochemical 'hotspots' of greenhouse gas (GHG) emissions, potentially enhancing positive feedback to climate warming by modifying regional to global carbon budgets (Walter *et al*. 2006; Schuur *et al*. 2008). This mechanism may have also been partly responsible for the global atmospheric increase in CH_4 during the last deglaciation (Walter *et al*. 2007a), although this subject is under debate (van Huissteden *et al*. 2011).

About 25% of the northern hemisphere land masses and more than 50% of Canada is affected by permafrost (Brown *et al*. 1998). In the northern Quebec-Labrador peninsula, permafrost is estimated to affect nearly one-third of the landscape, and a significant part of it at its southern limit is considered as warm permafrost, or near the thawing threshold of frozen ground (Allard & Seguin 1987). Along the eastern shore of Hudson Bay, the recent increase in air/ground temperatures and snow cover has contributed to the widespread reduction of permafrost areas along a north–south

DOI 10.1111/bor.12000

gradient: from less than 25% up north (58°N; Vallée & Payette 2007) to more than 80% in southeastern Hudson Bay (56°N; Payette *et al*. 2004). Thermokarst systems therefore occupy an increasingly significant surface area of subarctic Quebec. However, their natural variability and temporal evolution, recorded in the bottom sediments, have yet to be characterized to assess their potential contribution to the regional and global biogeochemical cycles at northern latitudes over a longer time frame.

In contrast to the lack of knowledge regarding thermokarst systems, diatoms (class *Bacillariophyceae*) are well established as sensitive recorders of palaeoenvironmental change. With their ubiquitous distribution and their rigid siliceous cell walls, diatoms are typically well preserved in lacustrine sediments and other aquatic/subaquatic environments. Moreover, several diatom species are highly sensitive to physical and chemical conditions in the water column (e.g. temperature, light availability, pH, dissolved organic carbon (DOC) and other chemical variables), making them valuable palaeolimnological indicators (Battarbee *et al*. 2002). Modern diatom assemblages collected from surface sediments of arctic/subarctic lakes have been used to develop transfer functions for the reconstruction of a variety of past limnological properties, such as temperature (Pienitz *et al*. 1995), pH (Weckström *et al*. 1997), lake depth (Moser *et al*. 2000) and DOC (Fallu & Pienitz 1999). Diatom–DOC relationships can provide useful insights into vegetation dynamics and climate change (Pienitz *et al*. 1999) or UV radiation in the water column (Pienitz & Vincent 2000). In thermokarst systems, Laurion *et al*. (2010) recently suggested that the direct influence of DOC on carbon transfer to the atmosphere (through microbial respiration and GHG emissions) may be less important than the effect of the chromophoric fraction of dissolved organic matter (CDOM), which strongly controls water temperature, thermal structure, and the availability of light and oxygen to the microbial communities. Their results suggest that the biogeochemical influence of organic-rich (i.e. peat) deposits around and underneath these ponds and of the organic matter produced *in situ* still has to be understood. Nevertheless, their study only represents a snapshot on short-term or present-day conditions and does not provide any information on the natural variability and temporal evolution of these systems. Palaeolimnological reconstructions of past DOC and CDOM conditions therefore could help to scale up such observations through time and space.

This study is part of a broader research initiative investigating past, present and future GHG emissions from thermokarst ponds in subarctic Quebec (Breton *et al*. 2009; Laurion *et al*. 2010; Bouchard *et al*. 2011; Watanabe *et al*. 2011). The overall objectives of the present study were (i) to describe the biostratigraphic properties of the sediments (i.e. diatom assemblages and pigment-related spectral properties) in limnologically differing ponds, and (ii) to reconstruct the palaeolimnological evolution (especially DOC) of these ponds over the recent past (last centuries). From a broader perspective, it provides the palaeolimnological background against which present-day conditions (e.g. geomorphology, biogeochemical cycles, optical properties) can be assessed. This work represents the biostratigraphic counterpart of a companion paper (Bouchard *et al*. 2011) dealing with lithostratigraphy and chronology. Here we present the results obtained from six ponds covering a relatively wide range of contrasting limnological properties (e.g. colour, transparency, dissolved and particulate component concentrations). Biostratigraphic properties of the sediments were examined by combining fossil diatom analysis with visible near infrared (VNIR) derivative spectroscopy of bulk sediment. To our knowledge, this is the first documented biostratigraphic study of small thermokarst ponds that resulted from the thawing of permafrost mounds at high latitudes, and therefore contributes to the growing literature on thermokarst pond dynamics.

Study site

The study site (55°20′N, 77°30′W, 105 m a.s.l.) is located in subarctic Quebec near the hamlet of Kuujjuarapik-Whapmagoostui, about 20 km inland from the eastern coast of Hudson Bay (Fig. 1). This small village (~1400 inhabitants) hosts adjacent Inuit (Kuujjuarapik; 'little great river' in Inuktitut) and Cree (Whapmagoostui; 'place of the beluga' in Cree) communities (Bhiry *et al*. 2011). It is situated on Precambrian rocks (granite and gneiss) that were strongly eroded by Pleistocene glaciations, the last one (Wisconsin) ending in the area around 8000 years ago when the Laurentide Ice Sheet (LIS) retreated northeastwards (Dyke & Prest 1987). The final break-up of the LIS was accompanied by the rapid final outburst of proglacial lake Agassiz-Ojibway (Veillette 1994; Barber *et al*. 1999; Lajeunesse & St-Onge 2008) and the formation of the Late Glacial Sakami moraine (Hillaire-Marcel *et al*. 1981). This deglaciation episode was followed by the postglacial Tyrell Sea transgression (*c.* 7900 cal. a BP), which covered the landscape up to present-day elevations of 250–300 m a.s.l. and left marine (silt–clay) and littoral (sand) deposits in topographic depressions (Hillaire-Marcel 1976; Saulnier-Talbot & Pienitz 2001). Postglacial emergence of the area occurred *c.* 6000 cal. a BP, and isostatic rebound is now estimated at more than one metre per century, one of the fastest rates in the world (Allard & Tremblay 1983).

The prevailing climate is subarctic. At the Kuujjuarapik-Whapmagoostui weather station

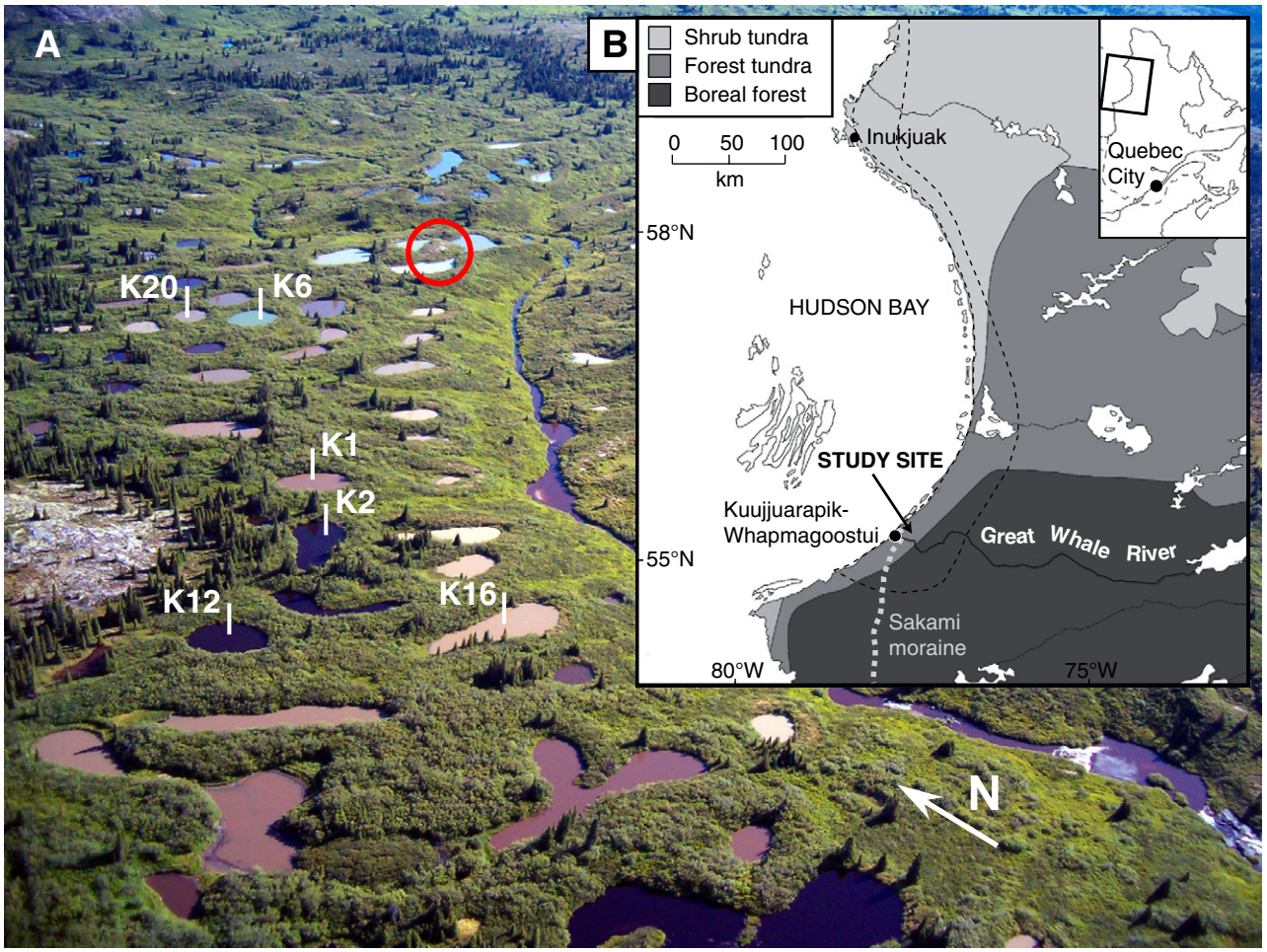

Fig. 1. Location of the study site. A. Oblique aerial photograph showing sampled ponds (numbers as in the text). The red circle shows the only permafrost mound (lithalsa) still present in the field (photo: F. Bouchard). B. Regional map showing the vegetation zones in subarctic Quebec. The black dashed line surrounds the northern part (Hudson Bay) of subarctic northwestern Quebec from which the diatom-DOC calibration dataset (inference model) was developed (Fallu & Pienitz 1999). The light grey dashed line represents the northern tip of the Lateglacial Sakami moraine, which marks the easternmost reach of proglacial lake Agassiz-Ojibway (Hillaire-Marcel *et al.* 1981). The study site (55°20′N, 77°30′W) is located near Kuujjuarapik-Whapmagoostui, along the Great Whale River.

(55°17′N, 77°45′W, 10 m a.s.l.), the mean annual air temperature is –4.4°C, ranging from monthly means of –23.4°C in January to 11.4°C in August (Environment Canada 2010). The annual freezing index (sum of degree-days below zero) is more than twice the thawing index (sum of degree-days above zero), i.e. 2890 versus 1310 respectively. Average annual precipitation is ~650 mm, with more than 35% falling as snow. The study area is located at the southern edge of the discontinuous and scattered permafrost zone, where frozen ground affects less than 50% of the land surface (mainly exposed hills and peatlands) (Allard & Seguin 1987).

The study site consists of a small peatland formerly affected by permafrost but now in an advanced degradation stage. The thawing of permafrost mounds (mainly lithalsas or mineral palsas) has resulted in the inception and development of several thermokarst ponds (Fig. 1). These ponds are generally round (10–30 m diameter) and shallow (1–3.5 m depth). In most cases, a 1–2 m high peripheral ridge covered by dense shrub and tree vegetation surrounds them. They are located in the upper section of a small valley that slopes to the south towards the Kwakwatanikapistikw River (local Cree name), a tributary of the Great Whale River. The landscape is relatively flat, but slight topographic and hydrologic gradients extend from the west owing to adjacent rocky hills and to the east owing to a steeply embedded creek. Based on sediment sampling of the peripheral ridges (F. Bouchard, unpublished data) and on former studies in the area (Arlen-Pouliot & Bhiry 2005; Bhiry & Robert 2006; Calmels *et al.* 2008), the marine sediments between and underneath the ponds are assumed to contain no permafrost. In fact, only one lithalsa, severely affected by thawing and surrounded by newly formed thermokarst ponds, is still visible on the site (Fig. 1).

Table 1. Morphological and limnological properties of sampled ponds.

		Pond number						Min	Max	Mean
		K2 black	K12 black	K6 green	K1 brown	K16 beige	K20 beige			
General morphology										
Max depth	m	3.0	2.7	3.5	2.3	2.3	2.7	2.3	3.5	2.7
Secchi depth	m	1.40	1.21	0.86	0.53	0.22	0.30	0.22	1.40	0.75
Surface area	m^2	470	365	385	390	635	220	220	635	411
UF thickness	cm	2.0	2.0	3.0	4.5	0.75	2.0	1.5	4.5	2.5
Limnology										
DOC	mg L^{-1}	5.9	6.9	3.8	7.6	8.7	7.7	3.8	8.7	6.8
TSS	mg L^{-1}	2.8	2.5	3.7	6.3	24.3	22.2	2.5	24.3	10.3
DOC/TSS		2.1	2.8	1.0	1.2	0.4	0.3	0.3	2.8	1.3
a_{320}	m^{-1}	21.1	27.2	8.3	32.7	35.7	32.7	8.3	35.7	26.3
K_{dPAR}	m^{-1}	1.8	2.0	1.4	2.6	4.9	4.4	1.4	4.9	2.8
pH		6.3	6.3	6.3	6.6	7.2	6.2	6.2	7.2	6.5
Temperature/oxygen profiles										
Temperature, surface	°C	16.4	19.4	20.0	18.9	24.3	22.3	16.4	24.3	20.2
Temperature, bottom	°C	8.5	7.9	10.6	7.7	7.1	4.5	4.5	10.6	7.7
Oxygen, surface	mg L^{-1}	8.1	9.1	9.2	9.6	9.3	9.1	8.1	9.6	9.1
Oxygen, bottom	mg L^{-1}	0.5	1.1	0.9	2.1	0.1	0.1	0.1	2.1	0.8

UF = upper facies (i.e. top lacustrine sediments in retrieved cores); DOC = dissolved organic carbon; TSS = total suspended solids; a_{320} = absorption coefficient by chromophoric dissolved organic matter at 320 nm; K_{dPAR} = diffuse attenuation coefficient for photosynthetically available radiation (PAR). Morphological and limnological properties were measured in July 2007 and July 2006, respectively. Methodology details are described in Laurion *et al.* (2010).

The vegetation cover in the study area is typical of the forest tundra zone in subarctic Quebec. Sparse trees and shrubs (e.g. *Picea mariana*, *P. glauca*, *Larix laricina*, *Ledum groenlandicum*, *Betula glandulosa*) are present on top of peripheral ridges, whereas poorly drained soils between the ponds are mostly covered by dense shrubs (*Salix* sp., *Alnus crispa*, *Myrica gale*), mosses (*Sphagnum* spp.) and herbaceous plants (e.g. *Carex aquatilis*). The studied thermokarst ponds show strikingly different limnological properties (Table 1), in particular regarding the DOC and total suspended solids (TSS) (for a detailed limnological description of these ponds and related methods see Breton *et al.* (2009), Laurion *et al.* (2010) and Watanabe *et al.* (2011)). Most of them are relatively humic and nutrient-rich ecosystems in which dissolved organic matter (DOM) is assumed to have a dominant allochthonous source (Breton *et al.* 2009). In spite of shallow water depths, these ponds are strongly stratified for most of the year, except during brief mixing episodes (fall overturn). They thus develop a seasonally hypoxic to anoxic hypolimnion, and are considered heterotrophic systems with largely supersaturated concentrations of dissolved CO_2 and CH_4 (Laurion *et al.* 2010).

Materials and methods

Field methods

Short sediment cores (length=10 to 20 cm) were taken in July 2007 in six thermokarst ponds covering a relatively wide range of limnological properties (Table 1). In addition to their differing colours, these ponds were selected for their accessibility during the relatively short (5–6 days) field campaign. The deepest part of each sampled pond was located with a portable sonar system, and at least two cores were collected with a 7-cm-diameter hand-held percussion corer (Aquatic Research Instruments). Sediment core lengths were restricted by the presence of a very sticky and compact clay unit underlying the recent lacustrine sediments (gyttja or organic mud). In order to prevent the mixing of the sediment–water interface, water from above the sediment surface was removed from the core tubes immediately after retrieval by drilling small holes through the coring tubes just above the sediment–water interface. The cores were then stored vertically for at least 48 h in non-freezing conditions, allowing the upper sediments to slowly consolidate by dewatering. The cores were sealed with floral foam blocks to minimize potential disturbances during subsequent transport. On arrival at the laboratory they were kept in the dark at 4°C.

Laboratory and statistical methods

Diatoms. – Sediment core liners were cut along their longitudinal axis with a rotating saw and split in half using a thin stainless steel wire. One core half was subsampled for lithostratigraphic analyses and chronology (Bouchard *et al.* 2011), while the other half was subsampled for biostratigraphic analyses (this paper). Before each subsequent analysis, altered or disturbed

sediment was removed from the split core faces by carefully running a stainless steel knife blade parallel to the sediment structures (laminations), when present. Split cores were visually described and photographed with a 500-dpi-resolution digital camera. They were then covered with a plastic film and kept in the dark (at 4°C) to minimize surface oxidation and desiccation.

Subsampling of the cores was done at 0.25 to 0.5 cm intervals for the surface sediments (top 4–5 cm) and at 0.5 to 1 cm intervals for the bottom sediments. Subsamples were freeze-dried for at least 48 h, depending on water content. Fossil diatoms were extracted using hydrogen peroxide (H_2O_2 30%) digestion techniques, mixed with marker microspheres of known concentration (0.386×10^6 microspheres mL^{-1}), and mounted on microscope slides using *Naphrax*, a highly refractive resin (Battarbee *et al.* 2002). For each subsample, a minimum of 400 to 500 diatom valves (or, when this was not possible because of very sparse diatom valves, a minimum of 1000 to 2000 microspheres) were counted along transects using a Leica DMRB light microscope. Identification was carried out to the lowest taxonomic level possible (i.e. species or variety/morphotype) at 1000× magnification. Taxonomic identification mainly followed Fallu *et al.* (2000) to be consistent with other studies conducted in the Hudson Bay region based on that flora (Fallu & Pienitz 1999; Ponader *et al.* 2002; Saulnier-Talbot *et al.* 2003); however, some supplementary taxa were identified using other floras (Krammer & Lange-Bertalot 1986, 1988, 1991a, b; Krammer 2000, 2002; Lavoie *et al.* 2008). In the following sections, taxon names are given as they appeared originally in consulted floras, and modern synonyms can be found in Table S1 (Supporting Information).

A striking contrast of diatom taxon diversity and absolute valve counts (more than 10-fold) was observed between the bottom and the surface of the analysed cores (the bottom being notably less rich in diatom valves than the surface). This could have resulted in a potential overrepresentation of the dominant taxa from the lower parts of cores if relative abundances had been plotted directly (only a few specimens of a given taxon representing nearly 50% of such levels, for example). To avoid this problem, relative abundances of the most common diatom taxa (i.e. those contributing to at least 5% of the total valve count in at least one sample) were multiplied by diatom/microsphere ratios (~1 near the surface, tending to less than 0.05 in the bottom sediments). For each core (pond), the normalized relative abundances were then plotted in stratigraphic diagrams using C2 software, version 1.5 (Juggins 2007). Stratigraphic zones were determined by Bouchard *et al.* (2011) following sedimentological, geochemical and chronological analyses (sediment facies). Diatom concentrations (number of valves per gram of sediment) were calculated using the total valve and microsphere counts (absolute values) and the microsphere concentrations. Diatom accumulation rates (DARs) (Anderson 1990; Wolfe 1997) were calculated using the abovementioned concentration data in conjunction with independently established sediment accumulation rates based on the ^{210}Pb chronology of each core (Bouchard *et al.* 2011).

A diatom-based inference model (Fallu & Pienitz 1999) was used to reconstruct past dissolved organic carbon (DOC, in mg L^{-1}) in thermokarst ponds. This model is based on the distribution of modern diatom assemblages in surficial sediments of 59 lakes from northwestern Quebec (including southeastern Hudson Bay, where the study site is located), through a latitudinal gradient spanning ~1100 km and ranging from the boreal forest (DOC values from 3.6 to 19.4, mean=9.8 mg L^{-1}) to the arctic shrub tundra (DOC values from 2.3 to 5.6, mean=3.7 mg L^{-1}) vegetation zones (Fig. 1). Because DOC measurements across the gradient are asymmetrical, they were log (x+1)-transformed for model calculation in order to normalize their distribution, and were then back-transformed (10^x–1) to obtain results in the original units (mg L^{-1}). Before using the model, a detrended correspondence analysis (DCA) (Hill & Gauch 1980) was performed on the fossil data (taxa representing at least 1% of the total valve count in at least one level) to determine if their principal floristic distribution pattern was similar enough to modern assemblages of Hudson Bay (Fallu *et al.* 2000). Diatom data (modern+fossil) were square-root-transformed, and a reduced statistical weight of 0.1 was attributed to fossil data. Levels with no analogue between modern and fossil data (i.e. fossil data not plotting among modern data 'clusters') were discarded. Hence the data from the lower facies (i.e. marine sediments; n=36) were not included in the DCA and the DOC model. DCA was performed using the software CANOCO, version 4.5 (ter Braak & Šmilauer 2002) and allowed to determine the compositional gradient lengths along each axis (>3 standard deviations (σ) for axis 1, and >2σ for axis 2), which confirmed the overlapping unimodal distribution of both modern and fossil diatom taxa. The chosen model is a five-component WA-PLS (Weighted Averaging Partial Least Square regression) with square-root transformation of species data, using the jack-knife re-sampling technique to calculate the associated error (Fallu & Pienitz 1999). This model has shown a strong relationship between modern diatom assemblages and DOC, with an $r^2_{(jack)}$ of 0.81 and a root mean squared error of prediction ($RMSEP_{jack}$) of 0.09 (0.23 mg L^{-1}). It was also used to infer past DOC concentrations in subarctic lakes elsewhere in eastern Hudson Bay (Ponader *et al.* 2002; Saulnier-Talbot *et al.* 2003).

Diffuse spectral reflectance. – Diffuse spectral reflectance (DSR) measurements were conducted for the VNIR wavelengths (400 to 2500 nm) on an Analytical

Spectral Devices (ASD) Labspec Pro FR (full range) using a high-intensity contact probe, equipped with a 2-mm spot size (Yurco *et al*. 2010). Results were originally reported at 2-nm resolution, but were averaged to 10-nm resolution to increase the signal-to-noise ratio. These spectra were extracted from sediment subsamples (0.25–0.5 cm interval), freeze-dried, and ^{210}Pb-dated in a companion sedimentological study (Bouchard *et al*. 2011). As VNIR reflectance spectra are sensitive to matrix grain size and water content, their spectral shape can be altered by scattering and absorption; thus, the derivative (rate of change) of each reflectance spectrum was calculated to minimize these effects. Reflectance derivative spectroscopy has been successfully used in marine geology to identify carbonate, iron oxide/oxyhydroxide, as well as clay and biogenic pigment fractions in sediments (Ortiz *et al*. 2004, 2009; Yurco *et al*. 2010).

A variable-based, varimax-rotated principal component analysis (VPCA) was performed on the visible part (400–700 nm) of these derivative reflectance spectra to provide orthogonal components that can be related to sediment composition (Ortiz 2011). Such component spectral signatures (i.e. component loadings plotted against wavelength) were compared with reference derivative spectra of various known standards to identify specific mineral and/or biogenic substances (pigments). Down-core variations of the dominant components (n=4) were plotted against sediment depth/age, together with other biostratigraphic data (e.g. diatom concentrations and accumulation rates). Because VNIR derivative spectroscopy data were available for only four ponds (K1, K2, K6 and K20), diatom abundances and other diatom-related results (e.g. diatom-inferred DOC) are presented here only for these ponds. However, supplementary information on the other two ponds (K12, K16) can be found in Figs S1–S6 and Tables S2–S3 (Supporting Information).

Results

General stratigraphy

All sediment cores can be separated into three contrasting facies (Fig. 2). The bottom sediments (lower facies (LF), >2–6 cm depth) do not show visible laminations or sedimentary structures, and appear dry and sticky with a dark grey colour. They are overlain by organic sediments (upper facies (UF), <2–4 cm depth to the surface) that are finely laminated (≤1 mm) and appear relatively soft and wet with a lighter greyish brown colour. The transition zone (TZ) between these two facies consists of millimetre- to centimetre-scale organic-rich horizons in the form of macroscopic peat/plant debris or thin dark brown to black layers. Detailed lithostratigraphic and chronological analyses of these sediment cores (Bouchard *et al*. 2011) revealed that (i) LF is considerably older and made of massive marine silts and clays deposited during the postglacial Tyrrell Sea transgression (*c*. 8000 to 6000 cal. a BP), which later emerged owing to glacio-isostatic rebound and were subsequently affected by permafrost inception and growth (*c*. 1500 to 400 cal. a BP); (ii) TZ probably represents the ancient peaty summits of permafrost mounds that were partially eroded and subsequently submerged; (iii) UF consists of organic-rich and humic lacustrine muds deposited since permafrost thawing and subsidence, hence since thermokarst pond inception (the last 150–200 years). These results were used to constrain the major biostratigraphic zones in the analysed cores. Unless otherwise specified, only UF and TZ are presented in the following sections, as there were almost no diatoms in the bottom sediments (LF) of analysed cores (see next section).

Diatom stratigraphy

A total of 108 diatom taxa belonging to 26 genera were identified for the whole set of cores (Table S1). Considering each pond separately, an average of 86 taxa (ranging from 69 to 95) per pond were identified (Table 2), among which nearly two-thirds (62%, ranging from 52 to 70%) represented more than one percent in at least one level. These taxa, accounting for ~95% (from 89 to 99%) of the total diatom abundance, were subsequently used in data ordination and inference model calculations. The proportion of taxa representing more than five and ten percent in at least one level appears more variable among ponds, with mean values of 27% (from 16 to 45%) and 17% (from 6 to 35%), respectively. Nevertheless, these taxa can account for a significant part of the total abundance. For example, ponds K6 and K20 show above average values with more than 90% (taxa >5%) and more than 80% (taxa >10%) of the total abundance. When only UF and TZ layers are considered, the five most abundant taxa in each core represent nearly half of the total abundances (48%, ranging from 33 to 58%). These dominant taxa are represented by the benthic genera *Achnanthes*, *Fragilaria*, *Nitzschia*, *Pinnularia*, *Frustulia* and *Navicula*, and by some planktonic/tychoplanktonic taxa (*Cyclotella* sp. and *Tabellaria flocculosa*). These taxa are preferentially either circumneutral to alkaliphilous (genera *Achnanthes*, *Fragilaria*, *Nitzschia*) or circumneutral to acidiphilous (genera *Pinnularia*, *Frustulia*, *Tabellaria*).

Relative abundances of diagnostic diatom taxa (corrected to diatom/microsphere ratios) are presented for the selected ponds in Fig. 3 (complete diagrams, including all taxa >5%, are presented in Figs S1–S6). The majority of identified taxa are benthic. Large-sized *Pinnularia borealis* specimens (as well as other *Pinnularia* taxa) appear modestly (<5%) in deeper layers (LF and TZ) of most analysed cores but are nearly absent from

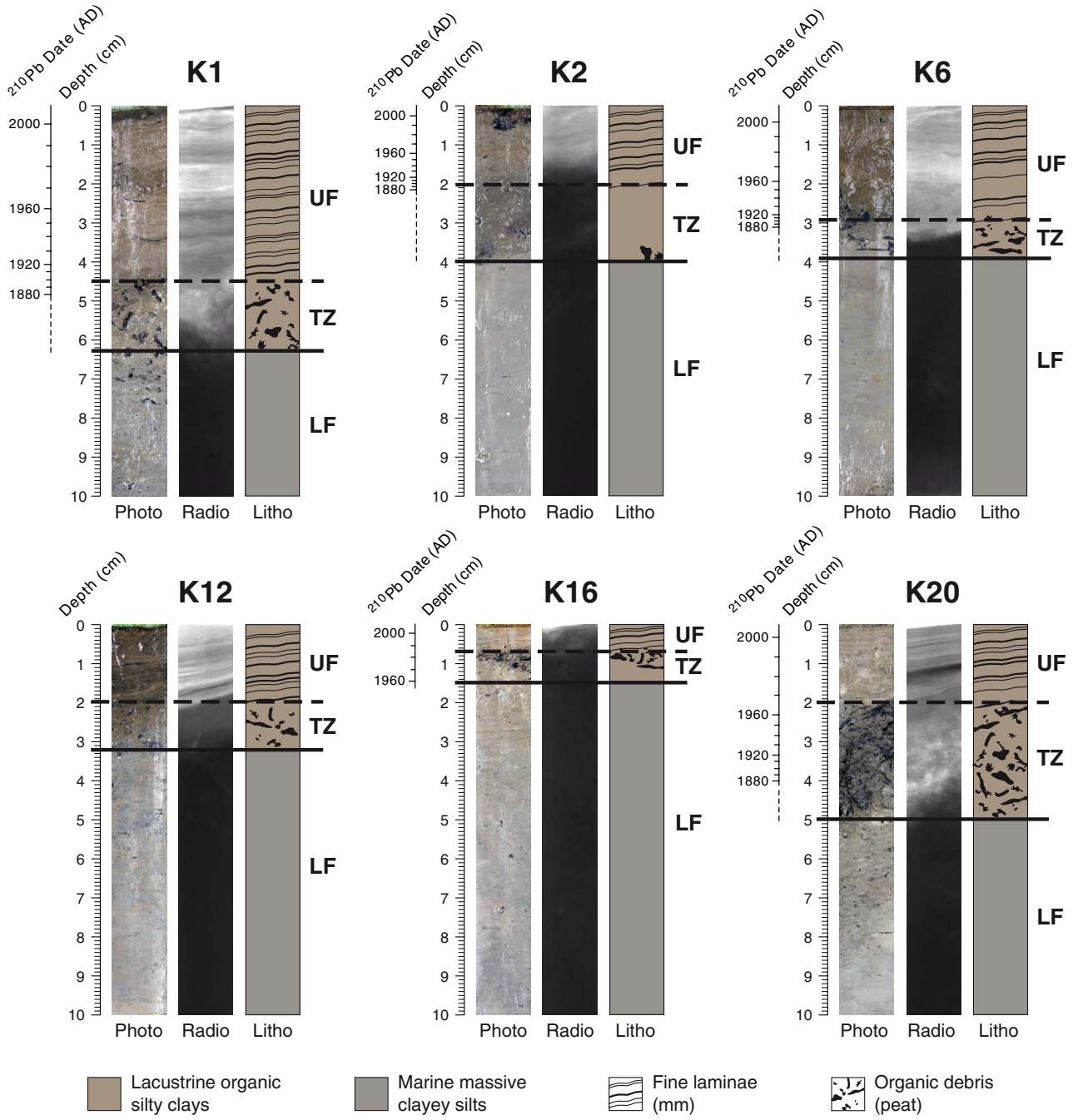

Fig. 2. General stratigraphy of sampled ponds. Photo = 500 dpi digital photograph; Radio = 16-bit greyscale micro-radiograph; Litho = simplified lithostratigraphy; UF = upper facies (lacustrine); LF = lower facies (marine); TZ = transition zone (peat and organic matter debris) between UF and LF. Unless otherwise specified, only UF and TZ were included in the biostratigraphic and derivative spectral analyses. Greyscale micro-radiographs (Radio) were previously acquired with an Itrax Core Scanner (Croudace *et al.* 2006), and methodology details are described in Bouchard *et al.* (2011).

the surface sediments (UF). In contrast, smaller taxa such as *Achnanthes pusilla* and *Fragilaria pinnata* are generally sparse to absent in LF and TZ, and their abundance increases sharply in UF. This trend is similar for *Nitzschia perminuta*, planktonic/tychoplanktonic *Tabellaria flocculosa*, and the majority of identified taxa (Figs S1–S6). In addition, normalized diatom abundances and diatom/microsphere ratios vary strikingly along studied cores. There are very few valves (and low taxon diversity) in lower levels, where diatom/microsphere ratios tend to be negligible, compared with UF layers, which show a much higher diversity and diatom/microsphere ratios of ~1. In this regard, some levels in LF revealed no more than a

Table 2. Summary of diatom counts, relative abundances and dominant taxa in studied ponds.

	Pond number					
	K2 black	K12 black	K6 green	K1 brown	K16 beige	K20 beige
Total counts						
Number of samples (levels)	9	23	21	22	9	39
Total number of taxa	83	85	86	95	69	95
Taxa >1%						
Number of taxa >1%	52	44	60	62	43	58
Percentage of taxa >1%	62.7	51.8	69.8	65.3	62.3	61.1
Total abundance of taxa >1%	92.5	95.9	99.1	94.7	88.8	96.7
Taxa >5%						
Number of taxa >5%	15	21	39	21	11	33
Percentage of taxa >5%	18.1	24.7	45.3	22.1	15.9	34.7
Total abundance of taxa >5%	65.1	87.1	91.7	66.7	61.1	92.0
Taxa >10%						
Number of taxa >10%	6	15	30	10	4	22
Percentage of taxa >10%	7.2	17.6	34.9	10.5	5.8	23.2
Total abundance of taxa >10%	37.5	78.8	83.0	41.4	36.5	80.6
Upper facies (UF) only						
Five most dominant taxa	FRAPINN	ACHMARG	ACHCFCU	FRABREV	ACHPUSI	ACHMARG
	NAVCRYC	FRAPINN	ACHPUSI	FRACOVE	FRACAPU	FRAPINN
	NITPER1	NAVCRYC	CYCSP00	FRAPINN	FRACOVE	NITGRAC
	PINBRAU	NITPER1	FRAPINN	FRUCFRH	FRAPINN	NITPER1
	TABFLOC	TABFLOC	NAVCRYC	PINNODO	NITPER1	TABFLOC
Total abundance	37.4	55.6	45.8	32.8	57.3	57.7

ACHCFCU = *Achnanthes curtissima*; ACHMARG = *Achnanthes marginulata*; ACHPUSI = *Achnanthes pusilla*; CYCSP00 = *Cyclotella* sp.; FRABREV = *Fragilaria brevistriata*; FRACAPU = *Fragilaria capucina*; FRACOVE = *Fragilaria construens* var. venter; FRAPINN = *Fragilaria pinnata*; FRUCFRH = *Frustulia rhomboides*; NAVCRYC = *Navicula cryptocephala*; NITGRAC = *Nitzschia gracilis*; NITPER1 = *Nitzschia perminuta* f. 1; PINBRAU = *Pinnularia brauniana*; PINNODO = *Pinnularia nodosa*; TABFLOC = *Tabellaria flocculosa*. Taxon names are given as they appeared originally in consulted floras, and modern synonyms can be found in Table S1 (Supporting Information).

few tens of diatom valves dispersed among several thousands of microspheres (Table S2). For this reason, only UF and TZ data were used for ordination, diatom accumulation rates and transfer functions (see next sections).

Data ordination and diatom-based reconstructions

The similarity between fossil diatom assemblages in thermokarst ponds (UF and TZ facies) and those from modern lacustrine sediments in northwestern Quebec is shown in the DCA scatter plots (Fig. 4). With the exception of pond K20, all data are generally concentrated in a relatively narrow cluster of points plotting near boreal forest sites located either in southeastern Hudson Bay or in northeastern James Bay regions (Fig. 1). For all analysed cores, DCA eigenvalues (λ) for axes 1 and 2 are near λ_1=0.46 and λ_2=0.16, with mean gradient lengths of 3.45 and 2.05 standard deviations (σ) respectively, thus confirming the unimodal distribution of diatom taxa (Hill & Gauch 1980). These two axes account for an average of 21% of the cumulative variance in the diatom assemblages, a relatively low percentage typical of data sets containing a large number of taxa and many zero values (i.e. for samples in which taxa are missing) (Stevenson *et al.* 1991; Pienitz *et al.* 1995). The detailed results for the first DCA axes are compiled in Table S3.

Diatom concentrations, accumulation rates (DAR) and inferred DOC are plotted as a function of depth in Fig. 5A. As mentioned above, diatom concentrations are much lower in TZ and increase significantly in the top few centimetres of analysed cores (UF), where taxon diversity and valve preservation are much higher. Coupled with independently established (^{210}Pb) sedimentation rates, these results show that diatom accumulation rates are generally lower in TZ levels than in UF levels (with the exception of pond K20, which shows a decreasing trend towards the surface). DOC absolute values differ among ponds, but they generally show a decreasing trend towards the surface (values <7.5 mg L^{-1} in surface levels), approaching modern values (Table 1), at least relative to each other (i.e. K6 having the lowest, followed by K2, and then K1 and K20).

VNIR stratigraphy

The component loadings as a function of wavelength (used to interpret the VIS derivative spectroscopic data) are plotted in Fig. 6. Four leading components can be identified from their comparison with reference

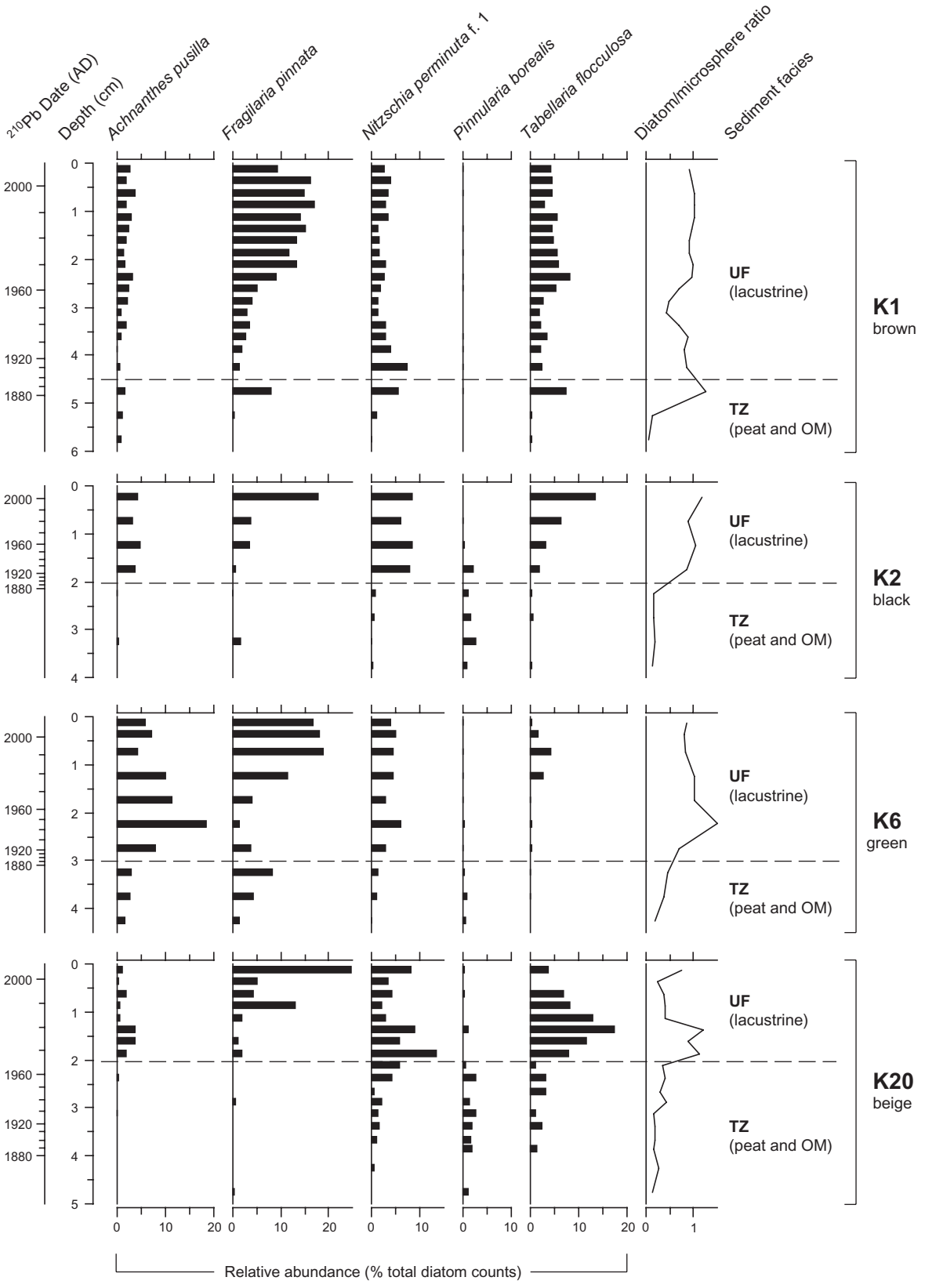

Fig. 3. Biostratigraphy of selected diatom taxa for four cores expressed as relative frequencies. UF = upper facies (lacustrine); TZ = transition zone (peat and organic matter debris) between UF and LF (lower facies, not shown). Complete diagrams of all analysed cores (n=6) are compiled in Figs S1–S6 (Supporting Information).

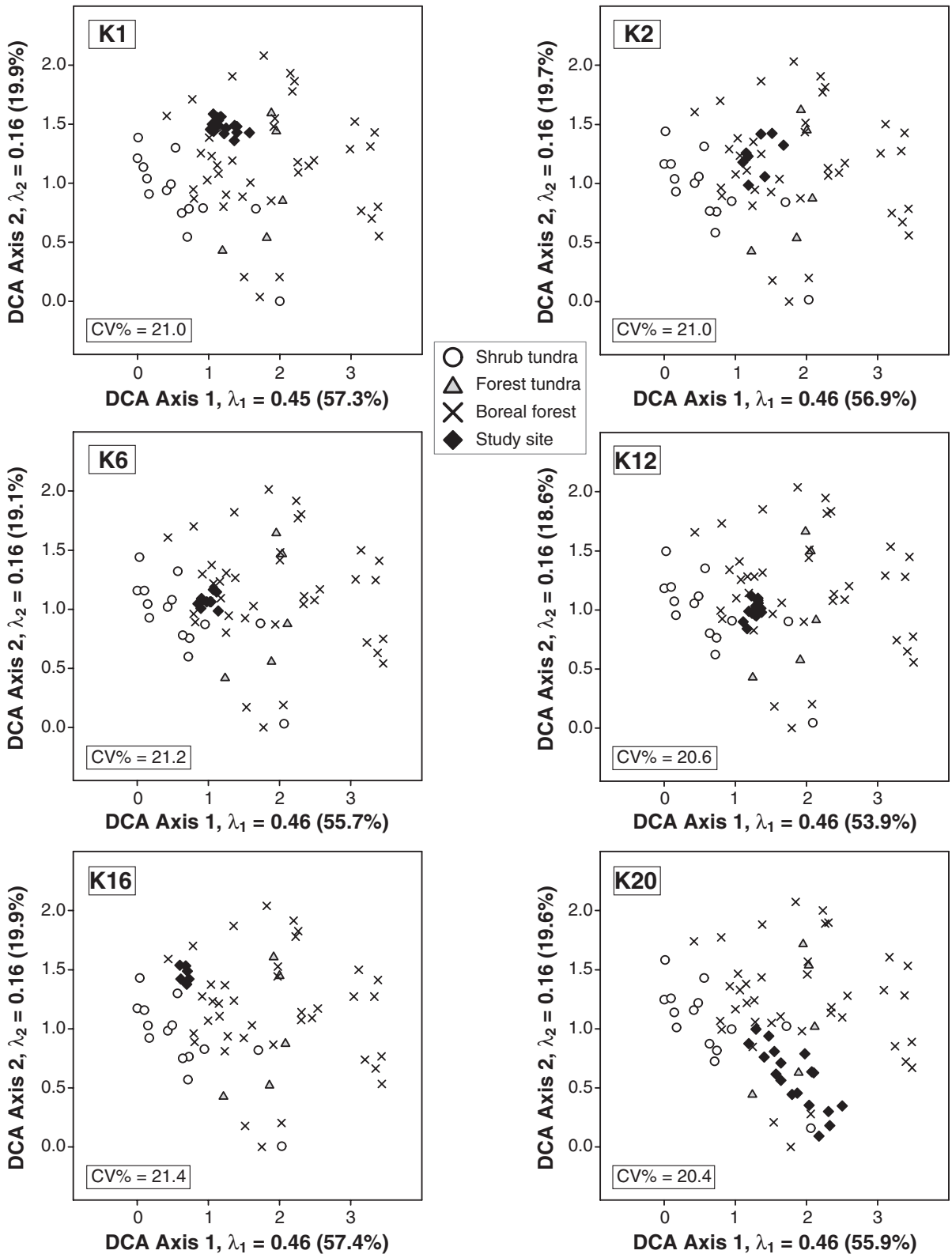

Fig. 4. Detrended correspondence analysis (DCA) for all analysed cores, comparing fossil diatom assemblages in thermokarst ponds near Kuujjuarapik-Whapmagoostui (filled diamonds) with modern assemblages in surface sediments from northwestern Quebec lakes (Fallu & Pienitz 1999), located in shrub tundra (open circles), forest tundra (grey triangles) and boreal forest (crosses) vegetation zones. Only data from the upper facies (UF) and transition zone (TZ) were included; data from the lower facies (LF) were discarded owing to a lack of overlap of taxa (see Materials and methods section for details). Detailed DCA results are compiled in Table S3 (Supporting Information).

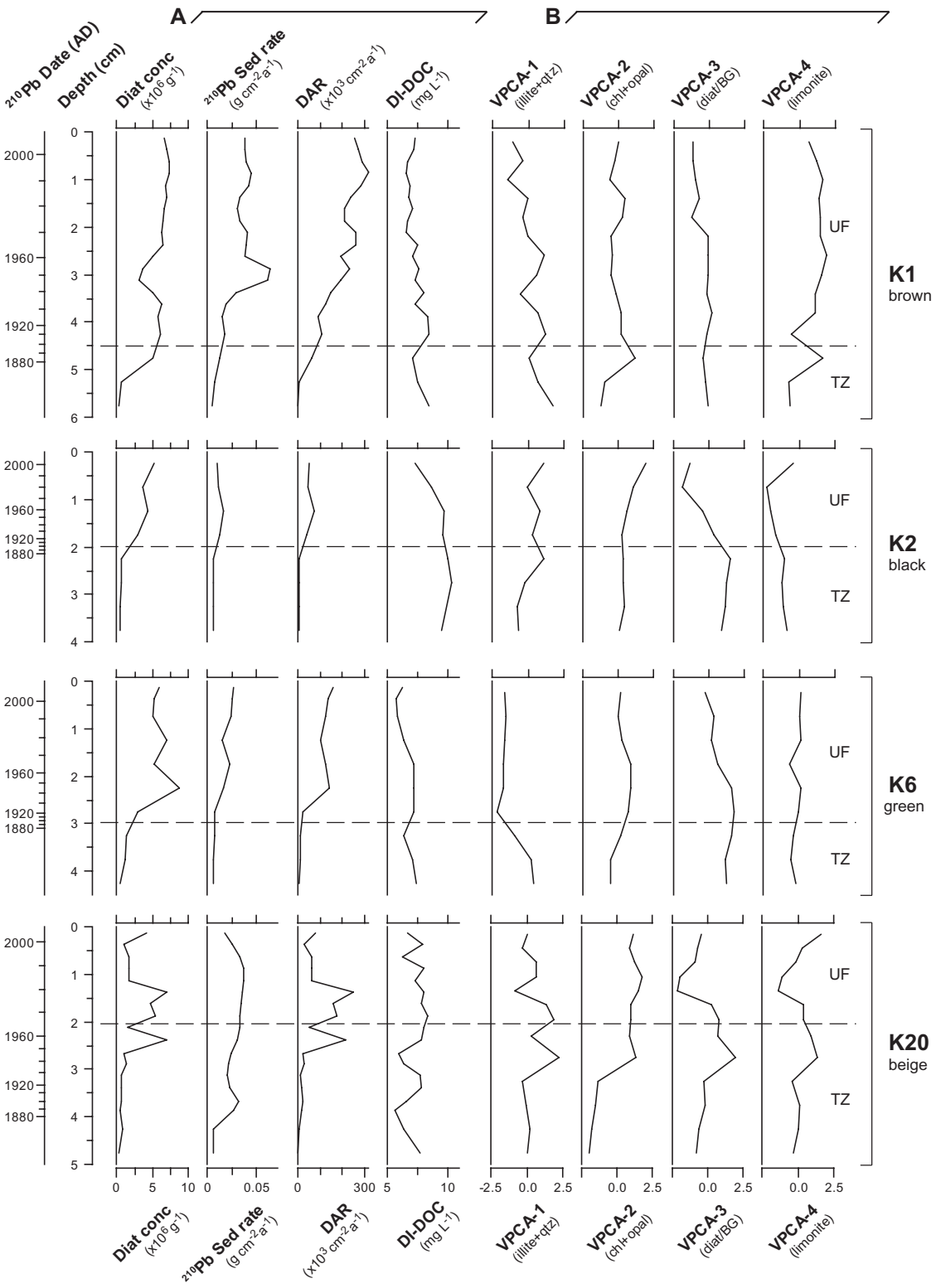

Fig. 5. Comparison between (A) diatom-derived data and (B) visible/near infrared derivative spectroscopy (VNIR) data, plotted as a function of depth/age. From left to right: Diat conc = diatom concentration ($\times 10^6$ cells g^{-1}); ^{210}Pb Sed rate = ^{210}Pb-derived sedimentation rate (g cm^{-2} a^{-1}); DAR = diatom accumulation rate ($\times 10^3$ cells cm^{-2} a^{-1}); DI-DOC = diatom-inferred dissolved organic carbon (mg L^{-1}); VPCA-1 = first component of varimax principal component analysis (illite+quartz); VPCA-2 = second component of varimax principal component analysis (chlorite+opal); VPCA-3 = third component of varimax principal component analysis (diatom/blue-green algae, inferred as eukaryotic/prokaryotic algae ratio); VPCA-4 = fourth component of varimax principal component analysis (limonite); UF = upper facies (lacustrine); TZ = transition zone (peat and organic matter debris) between UF and LF (lower facies, not shown).

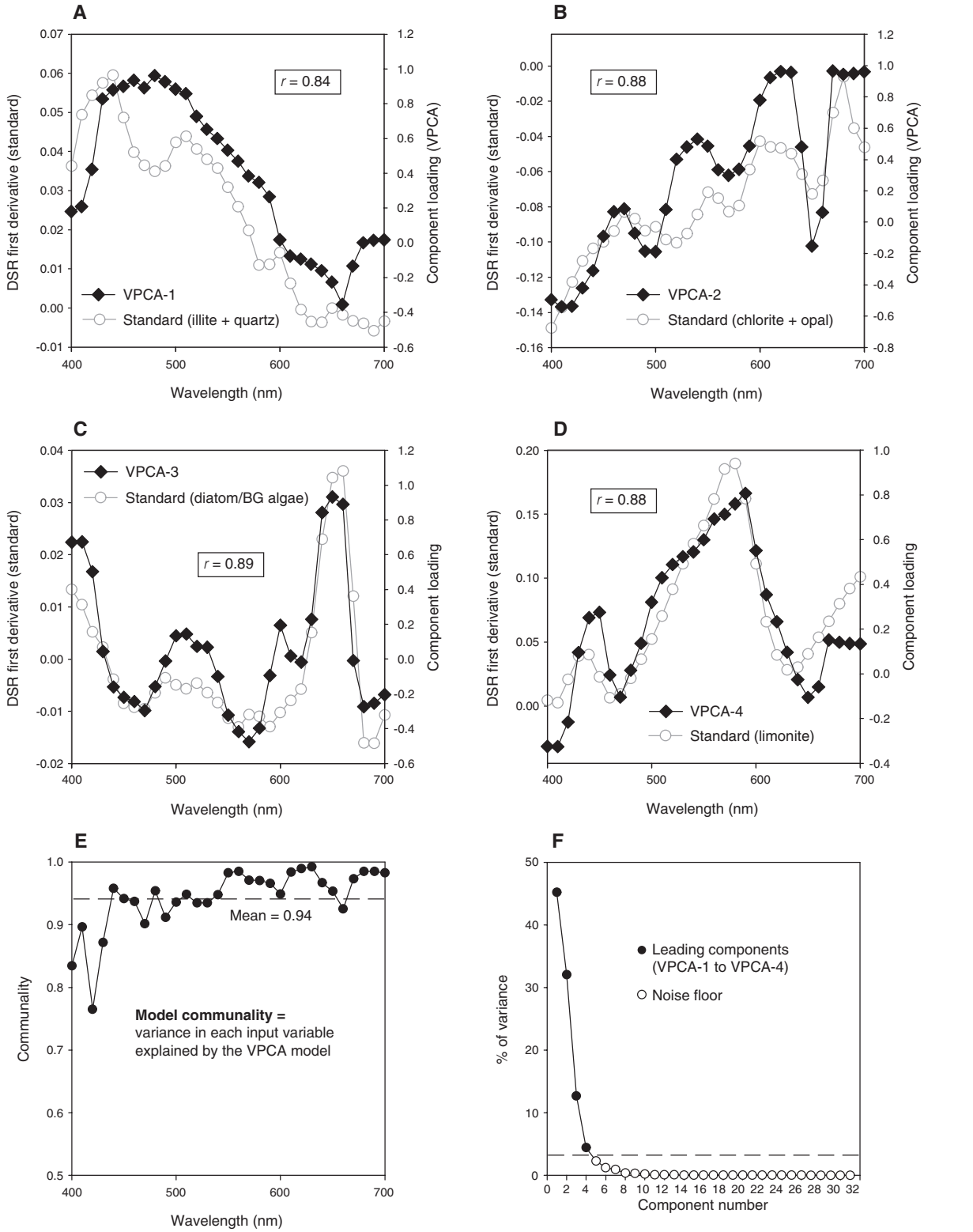

Fig. 6. A–D. Reflectance signatures of varimax-rotated component loadings and known standards plotted as a function of wavelength. A. First component (VPCA-1) vs. illite+quartz, r=0.84. B. Second component (VPCA-2) vs. chlorite+opal, r=0.88. C. Third component (VPCA-3) vs. diatom/blue-green algae, inferred as eukaryotic/prokaryotic algae ratio, r=0.89. D. Fourth component (VPCA-4) vs. limonite, r=0.88. E. Model communality, i.e. fraction of variance (from 0 to 1=from 0 to 100%) in each input variable explained by the varimax-rotated components extracted from the data set. F. Eigenvalues of each component scaled as the percentage of variance explained plotted as a function of component rank ('scree plot'), including the leading four components (filled circles) and the 'noise floor' (open circles). More details can be found in Table S4 (Supporting Information).

derivative spectra of known standards: the first component (VPCA-1) is correlated with the reflectance signature of an illite+quartz assemblage, with a correlation fit of r=0.84; VPCA-2 is correlated with the chlorite+opal signature, with r=0.88; VPCA-3 is correlated with the signature of the contrast between diatom and blue-green algae pigment spectra (r=0.89), which we infer to measure the ratio of eukaryotic to prokaryotic algae in the ponds; and VPCA-4 is correlated with the goethite+hematite (referred to as limonite) signature, with r=0.88. Each of these four correlations shows 28 degrees of freedom (d.f.) and a significance level (p) under 1% (p<0.01). Communality (i.e. how much variance in the original VIS derivative spectra is explained by the model as a function of wavelength) fluctuates around a mean value of 0.94 and is generally higher than 0.9 (except for a few lower values at shorter wavelengths), so that the model explains >90% of the variance (Fig. 6E). The four leading components account for 94% of the cumulative variance in the data set, ranging from ~45% for VPCA-1 to ~4% for VPCA-4 (Fig. 6F). The total percentages of variance explained by each component before and after varimax rotation are compiled in Table S4.

The VPCA component scores as a function of depth and age are presented in Fig. 5B, for comparison with the diatom abundance variations. VPCA-1 (illite+quartz) appears highly variable between ponds: generally decreasing in the upper facies of cores K1 and K20, increasing in the upper facies of core K2, and very stable and low in the upper facies of core K6. As a result, different VPCA-1 curves against depth do not clearly correlate with other diatom-related data (Fig. 5A). In contrast, VPCA-2 (chlorite+opal) shows a more synchronized trend with diatom concentrations, namely reaching higher values near the boundary between UF and TZ (K1, K6, K20) or closer to the surface (K2). VPCA-3 (eukaryotic/prokaryotic contrast) follows a less clear trend, but values are generally lower in surface sediments than near the UF–TZ boundary, being inversely correlated with diatom concentrations and accumulation rates. Finally, VPCA-4 (limonite) shows maximal values near the UF–TZ boundary (K1, K6), near the surface (K2) or in both horizons (K20).

Discussion

Paucity of fossil diatoms in the marine facies

Diatom abundances show a striking increase from the bottom to the surface. This trend is clearly observable in diatom/microsphere ratios of negligible values (>0.05) in LF that quickly increase to ~1 in UF (Fig. 3). Almost no fossil diatoms (or very few, i.e. <50 valves per level) were identified in LF, and these were freshwater rather than marine taxa (e.g. *Caloneis bacillum*, *Frustulia rhomboides*, *Navicula* (*Diadesmis*) *contenta*, *Pinnularia borealis*). In addition, valves found in these levels were often partly altered, broken or dissolved. These findings may challenge the marine origin of LF (as opposed to a proglacial lake origin, see below) formerly confirmed by sedimentological, geochemical and chronological analyses in the same cores (Bouchard *et al*. 2011). However, such an absence of marine fossil flora/fauna has also been reported from postglacial marine deposits along the southeastern (Hillaire-Marcel 1976) and eastern (Calmels *et al*. 2008; Lajeunesse 2008) coasts of Hudson Bay. Among proposed explanations, the very turbid nature (reducing light to extremely low values) of meltwater draining retreating inland ice masses (*c*. 6000 cal. a BP) may have precluded the development of aquatic biota in shallow coastal waters at that time. Indeed, light availability is a major regulator of algal productivity, through its definition of the limits of the euphotic zone.

Because some freshwater diatoms (although very sparse) were observed in LF, one could also propose a proglacial lake origin for these sediments. Lateglacial moraine deposits (the Sakami moraine), representing the eastern boundary of proglacial lake Agassiz-Ojibway in the James Bay and southeastern Hudson Bay regions, composed of rhythmic silts and clays devoid of fossil flora/fauna were indeed observed near Kuujjuarapik-Whapmagoostui, at ~5 km east of the Great Whale River mouth (Hillaire-Marcel 1976; Hillaire-Marcel *et al*. 1981). However, these morainal deposits are located several kilometres (>10 km) west of our study site, and glacial lake sediments are absent east of the Sakami moraine. Moreover, lateglacial deposits are separated from the overlying postglacial marine sediments (Tyrrell Sea) by a relatively thick (~20 cm) coarse sand unit containing up to 10–15% carbonate fragments (Hillaire-Marcel 1976). This sandy unit was not observed at our study site. For all these reasons, the proglacial lake hypothesis seems an unlikely explanation for the presence of freshwater diatoms in LF.

One must also consider the notable time gap between LF deposition (ending at postglacial emergence of the region some 6000 years ago) and its 'preservation' by permafrost inception, which possibly did not initiate until 3200 cal. a BP, but more probably around 1500 cal. a BP near the study site (Allard & Seguin 1987). This would leave 3000 to 4500 years during which these sediments must have been exposed to several surface processes, such as (i) peatland vegetation/soil establishment in the surroundings, driving an environmental shift to more acidic conditions and explaining the substantial drop in calcium (Ca) and strontium (Sr) XRF values observed by Bouchard *et al*. (2011) (Table 3); (ii) complete salt leaching of soils, explaining the negligible pore-water salinity observed by Calmels *et al*. (2008) in similar deposits; and (iii) partial destruction/dissolution

Table 3. Summary of lithostratigraphic and biostratigraphic data. ACHPUSI = *Achnanthes pusilla*; FRAPINN = *Fragilaria pinnata*; FRUCFRH = *Frustulia rhomboides*; PINBORE = *Pinnularia borealis*.

Lithostratigraphy (Bouchard *et al.* 2011)			Biostratigraphy (this paper)
Chronology	Sedimentology	Geochemistry	Diatoms
Upper facies (UF)			
c. 150 cal. a BP to recent (permafrost thawing/subsidence)	Lacustrine silty clays Finely laminated High water and organic content Low density No sand grains	Low detritic inputs (K, Si, Ti) Low redox-sensitive elements (Fe, Mn) (Seasonal hypoxia-anoxia) Variable pH-sensitive elements (Ca, Sr) Low global concentration	High diversity and concentration Freshwater, mostly benthic Circumneutral-alkaliphilous Low-DOC taxa (e.g. FRAPINN, ACHPUSI)
Transition zone (TZ)			
c. 500 to *c.*150 cal. a BP (ancient summits of palsas)	Peat and organic debris Chaotic structure High water and organic content Low density Few sand grains	Shift in detritic inputs (K, Si, Ti) Peaks in redox-sensitive elements (Fe/Ti) (Well-oxygenated water) Shift in pH-sensitive elements (Ca, Sr) Shift in most elements	Low diversity and concentration Freshwater, benthic and aerophilous Circumneutral-acidophilous High-DOC taxa (e.g. FRUCFRH, PINBORE)
Lower facies (LF)			
7900 to *c.* 6000 cal. a BP (postglacial Tyrrell Sea)	Massive marine clayey silts Low water and organic content High density Matrix-supported sand grains	High detritic inputs (K, Si, Ti) High redox-sensitive elements (Fe, Mn) High pH-sensitive elements (Ca, Sr) High global concentration	Almost no diatoms Freshwater, benthic and aerophilous Broken and/or dissolved valves Similar to TZ taxa, but scarce

of fossil remains by weathering or surface runoff, explaining the scarcity of diatom valves observed in LF. Finally, permafrost/thermokarst-related processes affecting silt and clay soils (e.g. frost heaving, extension cracking, gelifluction, cryo-desiccation and consolidation, thaw settlement) and occurring during the last several centuries may have disturbed the upper LF deposits, allowing for the incorporation of UF and TZ taxa along a network of freeze/thaw-derived narrow fractures (Konrad & Seto 1994; Calmels & Allard 2008). As shown by diatom diagrams including all sedimentary facies (Figs S1–S6), some of the diatom taxa observed in TZ and the lower part of UF as relatively intact specimens (e.g. *Frustulia rhomboides*, *Caloneis bacillum*, *Pinnularia* spp.) were indeed observed in LF, although very sparsely and as partly dissolved/broken specimens.

Are thermokarst ponds representative of other subarctic freshwater ecosystems?

Among the major factors controlling diatom assemblage composition, pH is often considered as the single most important in freshwater lakes (Battarbee *et al.* 2002) and rivers (Grenier *et al.* 2006). Many chemical or biochemical processes involved in diatom ecology are indeed pH-controlled, such as the balance between carbonic acid, carbonate and bicarbonate, the solubility of toxic metals (e.g. aluminium), and the availability of nutrients. This strong relationship has encouraged the development of a pH-related classification of diatom taxa (i.e. acidiphilous, circumneutral or alkaliphilous), widely used in biostratigraphic studies. In the absence of a modern diatom–pH calibration data set enclosing our study area, we must rely on a qualitative interpretation using the pH optima reported from geologically comparable subarctic sites (Weckström *et al.* 1997). However, fossil diatom assemblages in subarctic thermokarst ponds do not appear to be first and foremost controlled by pH. In some sediment cores (e.g. K1, K20), alkaliphilous taxa such as *Fragilaria pinnata* (pH optimum >7.0) were more abundant near the surface, while acidiphilous taxa such as *Frustulia rhomboides* (pH optimum <6.5) dominated within/near TZ; however, this trend was not that clear in other cores (e.g. K2, K12), where both acidiphilous taxa (e.g. *Tabellaria flocculosa*, *Pinnularia* spp.; pH optimum <7.0) and alkaliphilous *Fragilaria pinnata* were more dominant in the upper part of UF than near TZ. In addition, several circumneutral or pH-indifferent taxa such as *Achnanthes marginulata* or *Stauroneis anceps* (pH optimum=7.0) have also shown variable trends (increasing or decreasing) along the cores. Therefore, the diatom–pH relationship, although explaining part of the observed changes, may not be the most important controlling factor in this kind of environment and is probably associated with other factors, such as substrate type and DOC (see Table 3 and text below).

To explain diatom assemblage composition, one could also propose an explanation involving the efficient attenuation of incoming solar radiation in the water column of thermokarst ponds by a combined influence of turbidity (expressed as TSS, associated with light scattering and absorption) and dissolved organic matter (expressed as DOC, associated with light absorption) (Watanabe *et al.* 2011), strongly controlling light attenuation (expressed as K_{dPAR}, diffuse attenuation coefficient for photosynthetically available

radiation) and the thermal and oxygenic stratification (Laurion *et al*. 2010). For example, pond K6 (green colour) shows the lowest K_{dPAR} (low DOC/low TSS, Table 1) and is colonized mainly by benthic taxa, with almost no planktonic diatoms observed in surface sediments (Figs 3, S3), even though this is the deepest of all sampled ponds. By contrast, ponds K2 and K12 (black colour) have a slightly higher K_{dPAR} (average DOC/low TSS), and their corresponding diatom abundance diagrams show a significant increase in planktonic/tychoplanktonic *Tabellaria flocculosa* near the surface (Figs S2, S4). However, ponds K16 and K20 (turbid beige colour) show the highest K_{dPAR} values (high DOC, very high TSS) and strongest stratification (temperature and oxygen contrast between bottom and surface), but their diatom assemblages do not differ radically from those of other ponds (Figs S5, S6), especially the black ponds (K2 and K12) and, to a lesser extent, the intermediate brown pond K1 (Fig. S1). Thus, the diatom–light–DOC relationship may not be simple and is probably biased by the significant influence of TSS on light availability in these systems, pointing to other local pond conditions and/or landscape heterogeneity that control diatom assemblages (e.g. vegetation, soils, topography).

We propose that the substrate type on which these mostly benthic/periphytic diatom communities grow may be a major controlling factor. The taxa that are often found in subarctic peatlands and generally considered as aerophilous/bryophilous (i.e. living in subaerial habitats, e.g. *Caloneis bacillum*, *Eunotia* spp., *Frustulia rhomboides*, *Hantzschia amphyoxis*, *Pinnularia borealis*) (Pienitz 2001) were observed predominantly within TZ, which is rich in peat/moss fragments or layers (for detailed macro-/microscopic descriptions, see Bouchard *et al*. 2011). The former pond/palsa surface occupied by bryophyte mats (e.g. *Sphagnum* spp.) thus probably determined the abundance of these taxa during the early stages of pond inception. In the uppermost core sections (surface sediments), identified taxa (genera *Fragilaria*, *Navicula*, *Stauroneis*, *Tabellaria*) are generally associated with truly aquatic conditions, reflecting the shift from peaty to lacustrine sediment substrates. This controlling effect of substrate probably acts in conjunction with other related factors, such as DOC and pH, which cannot be ruled out as explanations of diatom assemblage composition (Table 3). However, such strong relationships between benthic/periphytic diatom communities and their substrate were also observed in a permafrost-patterned (ice wedges and polygons) wetland in the Canadian Arctic (Ellis *et al*. 2008), where aerophilous taxa (e.g. *Pinnularia borealis*) dominated on dry high-/low-centre polygons, while taxa typical of truly aquatic conditions (e.g. *Fragilaria* spp., *Navicula* spp.) dominated within lacustrine sediments of polygon ponds and thaw (thermokarst) lakes. Moreover, species diversity in this arctic landscape was found to be low during drier 'aerophilic' episodes (with only a few taxa such as *Pinnularia borealis* dominating the assemblages), but considerably higher when fully lacustrine conditions prevailed. The same pattern was observed in the fossil assemblages of the subarctic thermokarst ponds of our study site (i.e. high diversity in UF but much lower diversity in TZ). These results underscore the major influence of autogenic (*in situ*) processes (e.g. local vegetation/soil development, peat accumulation and erosion), in addition to allogenic forcing mechanisms (e.g. precipitation, geochemical leaching of glacial and marine sediments in the surroundings), on diatom community changes in the recent past.

A decreasing trend in diatom-inferred DOC

DOC values inferred from fossil diatom assemblages in thermokarst ponds ranged between about 5 and 10 mg L^{-1} (Fig. 5A). These results are typical of the forest tundra (2.7 to 6.5, mean=4.8 mg L^{-1}) and boreal forest (3.6 to 19.4, mean=9.8 mg L^{-1}) vegetation zones in subarctic Quebec (Fallu & Pienitz 1999). It is worth noting that the DOC model selected was originally developed based on modern assemblages in subarctic lakes showing different limnological conditions from those observed in thermokarst ponds (e.g. regarding lake surface, water depth, and large influence of TSS on transparency). Using the same transfer function to reconstruct past DOC in a subarctic lake near Kuujjuarapik-Whapmagoostui (about 8 km west of our study site), Saulnier-Talbot *et al*. (2003) found increasing DOC concentrations coinciding with vegetation (especially spruce) establishment in the catchment, along with higher allochthonous DOC inputs (mainly as fulvic and humic acids) to the lake. One would thus expect a similar trend, with recent vegetation establishment and growth around thermokarst ponds. However, the model rather showed a decreasing DOC trend (Fig. 5A), as illustrated by the predominance of high-DOC (>8 mg L^{-1}) diatom taxa (e.g. *Frustulia rhomboides*, *Pinnularia borealis*) in TZ and the lower part of UF, low-DOC (<6 mg L^{-1}) taxa (e.g. *Fragilaria pinnata*, *Achnanthes pusilla*) in surface sediments, and medium-DOC (6–8 mg L^{-1}) taxa (e.g. *Nitzschia perminuta*, *Tabellaria flocculosa*) between these levels (Fallu & Pienitz 1999). It is worth noting that these changes in inferred DOC may also be associated with changing pH conditions, as some high-DOC diatom taxa (e.g. *Frustulia rhomboides*) can also be considered as acidophilous, whereas some low-DOC species (e.g. *Fragilaria pinnata*) have more alkaline preferences (Table 3).

These apparently counterintuitive results may be associated with the variable impact of peat patches at thermokarst pond inception, the apparently small catchments of these ponds, and the influence of fine

mineral particles (accounting for the largest part of TSS) eroded from their littoral zones. Discontinuous, organic-rich moss layers were found in almost all analysed cores within the transition zone between the upper and lower facies (Fig. 2). These layers were interpreted as the remains of permafrost mound (palsa/lithalsa) summits partially eroded and subsequently submerged (owing to permafrost thawing and ground subsidence) during thermokarst pond inception (Table 3) (Bouchard *et al*. 2011). As a consequence, these peat layers represented a major source of *in situ* DOC for the carbon pool of newly formed ponds, resulting in high DOC concentrations in the water column at that early stage. DOC concentrations then may have decreased as dissolved organic molecules were adsorbed on abundant settling fine mineral particles (inorganic marine silts and clays), progressively 'capping' (i.e. isolating) the initial peat layers from the water column. The adsorption of DOC from different humic sources onto clay minerals has been demonstrated by Tietjen *et al*. (2005). This mechanism could explain the inferred decreasing DOC trends over time if the allochthonous input from a limited catchment remained of minor importance even though vegetation was growing in the surroundings, as seen on aerial photographs (F. Bouchard, unpublished data). Moreover, with limited new inputs, microbial degradation of the *in situ* DOC pool might have contributed to this decreasing trend.

Thick peat deposits have not been observed at the study site, and the only remaining permafrost mound is a mostly mineral mound (lithalsa) without a well-preserved organic cover (Fig. 1). However, several permafrost mounds in the forest tundra zone of Hudson Bay were first formed as palsas (i.e. peat-covered), and later evolved as lithalsas as their organic cover was eroded, suggesting a morphogenetic continuum between these two periglacial landforms (Pissart 2002; Calmels *et al*. 2008). As indicated by the organic-rich layers in the core transition zones (Fig. 2), it is highly probable that not all peat was eroded away. Moreover, palsa fields containing thick peat deposits (>2 m) are still present in the region, only a few kilometres away from the study site and at a comparable elevation (Arlen-Pouliot & Bhiry 2005; Bhiry & Robert 2006). It is thus likely that these peatlands extended over a larger area (including the study site) in the recent past, providing a significant source of organic matter in newly formed thermokarst ponds.

The very small extent of thermokarst pond catchments, limited to the inner part of the peripheral ridges (few square metres), may also support the above explanations. The fact that the surfaces were restricted, albeit densely colonized by vegetation (mosses, lichens, shrubs and sparse trees), meant that they contributed little in terms of allochthonous carbon inputs to pond waters. Thus, the local carbon budget may have fluctuated mainly in response to the aforementioned processes. It is worth noting that some breaches were present in several peripheral ridges, potentially allowing a restricted and mostly seasonal (spring) hydrological connection between some ponds (F. Bouchard, unpublished data). The existence of such connections could influence DOC balance in thermokarst ponds. However, more detailed hydrological investigations (e.g. using water stable isotope tracers such as ^{18}O and ^{2}H (Turner *et al*. 2010)) are needed to identify and quantify these hydrological networks and their impact. More generally, such links between ancient peat deposits and DOC trends, although difficult to disentangle, would be better quantified with more coring sites at each pond.

VNIR measurements in lacustrine sediments as a complement to diatom analysis

The down-core patterns observed in the VPCA component scores, although not clearly correlated with all diatom-related profiles (diatom concentrations and accumulation rates, diatom-inferred DOC), have revealed several indirect relationships with some diatom-inferred data (Fig. 5). These results demonstrate the complexity of subarctic thermokarst pond habitats, and suggest the relevance of using VNIR spectroscopy to complement biostratigraphic analyses of lacustrine sediments. First, VPCA-1 (illite+quartz) does not correlate with other diatom-related data, and may rather be related to internal bulk sediment production and deposition (i.e. turbidity). Indeed, pond turbidity (reported as TSS) is significantly different among ponds and appears to be related to reducing conditions in bottom waters resulting from a strongly stratified water column (e.g. in ponds K16 and K20; Table 1). However, this VPCA component does not correlate with silicon (Si), titanium (Ti) or potassium (K) curves (XRF values, data not shown) (Bouchard *et al*. 2011), elements usually found in fine detrital material such as silts and clays. This result supports the idea that steep temperature and oxygen gradients between surface and bottom waters are related not primarily to allochthonous mineral inputs alone, but also to dissolved organic matter, which strongly controls light attenuation as mentioned above (Watanabe *et al*. 2011). The relationships may also be overridden or masked by organic or peat layer-related signals (see previous section). Second, VPCA-2 (chlorite+opal) shows a more synchronized trend with diatom concentrations, as reflected by higher values near TZ (ponds K1, K6 and K20) or closer to the surface (pond K2) for both proxies (Fig. 5). This link is obvious as diatoms frustules are made of opal (amorphous or noncrystalline silica). Moreover, this component generally shows opposite trends along the cores compared with VPCA-1 (illite+quartz), and is inversely correlated with

several detrital elements (see below). Again this is a logical relationship because diatoms, although not particularly abundant in such high-latitude environments ($5–10\times10^6$ cells g^{-1}), probably represent the main component of the sediment biogenic fraction that is fluctuating in response to its lithological counterpart (i.e. the relative proportion of the former being directly affected by the dilution of the latter, and *vice versa*). Third, VPCA-3 (eukaryotic/prokaryotic algae) is generally lower in surface sediments than it is near the UF–TZ boundary, and thus is inversely correlated with overall diatom concentrations and accumulation rates. This may reflect the progressive appearance of prokaryotic cyanobacteria as anoxic/hypoxic conditions developed in bottom waters (hypolimnion), as proposed by Bouchard *et al*. (2011) based on lithostratigraphic evidence (peaks in redox-sensitive Fe/Ti ratio curves from XRF data; Table 3). Finally, VPCA-4 (limonite) generally shows minimal values near the UF–TZ boundary and/or near the surface, which is probably related to the oxidation state (redox conditions) of the sediments as anoxic/hypoxic conditions developed in bottom waters. As mentioned above, such episodes were also inferred for comparable depths from sedimentological and geochemical data generated for the same ponds.

To investigate further how the down-core VPCA components correlate with sediment composition variability among the studied ponds (especially the biogenic fraction), we compared the VNIR spectral data with individual diatom taxa identified in this study. The results showed several significant relationships ($p<0.01$) between VPCA components and diatom data at the taxonomic level (Table S5). For example, epipelic *Amphora libyca* and *Caloneis bacillum* (abundant in lacustrine muds) were strongly correlated with the turbidity component (VPCA-1). On the other hand, the diatom component (VPCA-2) was found to be inversely correlated with a few diatom species/genera (including epipelic *Caloneis bacillum*), but especially with a broad suite of lithologic elements measured by XRF (Bouchard *et al*. 2011). This confirms the generally opposite trends along the cores for this component compared with VPCA-1, as discussed above and shown in Fig. 5. In addition, VPCA-3 (eukaryotic/prokaryotic algae) and VPCA-4 (limonite), both related to redox conditions (anoxia/hypoxia development) in bottom waters, showed both direct and inverse correlations with specific diatom taxa, some of which are among the most abundant diatoms (e.g. *Fragilaria construens* var. *venter*). The aforementioned relations, although complex and difficult to disentangle from all other environmental factors, confirm that the reflectance VNIR data show similarity to both geochemistry and diatom data at the taxonomic level.

The VNIR approach, which consists of acquiring diffuse reflectance spectra in the visible and near infrared wavelengths (400 to 2500 nm) and transforming these into multivariate statistical data (VPCA components), has been used with success in palaeoceanography (Ortiz *et al*. 2004, 2009; Yurco *et al*. 2010; Ortiz 2011) and palaeolimnology (von Gunten *et al*. 2009; Debret *et al*. 2011) to identify key sources and transport pathways of mineral/biogenic deposits in various sedimentological settings. To our knowledge, this technique had not yet been used in conjunction with biostratigraphic analyses (e.g. diatoms). We thus believe that VNIR derivative spectroscopy has the potential to complement and improve multiproxy studies in subarctic and arctic thermokarst systems in the future. To set the scene for such forthcoming work, we present in the following paragraph some potential links between surface sediment biostratigraphic properties (diatoms and VNIR derivative spectra) and limnological properties of the water column, providing insights into the biogeochemistry of thermokarst ponds.

Comparison of the VNIR spectral analysis measurements from surface sediment in each of the four ponds provides some interesting correlations when plotted against selected limnological and diatom data (Fig. S7). While we must be careful when interpreting these correlations because of the small sample size ($n=4$), the results from this preliminary analysis are nevertheless consistent with the independent estimates of the VPCA component loadings (Fig. 6). We therefore limit our discussion to highly significant correlations with coefficients ≥0.95 that show clear linear relationships. A more complete comparison of the VNIR data with the other measured proxies (including diatom-inferred data) is provided in Table S6. First, the leading two VPCA components (VPCA-1, illite+quartz and VPCA-2, chlorite+opal), which relate to the sediment composition and are strongly linked at the surface ($r>0.97$; $p<0.05$), are significantly correlated with the pH contrast between the epilimnion and hypolimnion ($r=–0.99$; $p<0.05$) and with the total number of diatom taxa ($r=–0.97$; $p<0.05$) (Fig. S7). As mentioned above for down-core VPCA component curves, these results are at least partly related to pond turbidity, and thus to thermal or oxygenic stratification resulting in less effective exchanges between surface and bottom waters. For example, the more stratified and turbid ponds (K1 and K20) show a higher pH contrast, pointing to less mixing with deeper waters. However, these ponds also show higher diatom diversity, as expressed by the total number of taxa. This inverse relationship between diatom diversity and VPCA-1 is possibly influenced by local properties such as the substrate type (as discussed above). It is worth recalling that peat debris or layers were found to be more abundant in highly turbid ponds (K1 and K20, showing lower VPCA-1 surface values) than in less turbid ponds K2 and K6 (Fig. 2). Second, VPCA-4 (limonite) is best correlated with the surface sediment diatom to bottom-water bacteria ratio

(r=0.94; p=0.06). This suggests that more oxic sediments (higher limonite concentrations) show a higher diatom/bacteria ratio, hence a better production and/or preservation of diatom valves. In contrast, more reduced sediments (lower VPCA-4) show a lower diatom/bacteria ratio, and thus enhanced bacterial activity in the bottom waters. The green pond (K6), with its less stratified and clearer water column (i.e. lower DOC, lower absorption coefficient a_{320} and lower attenuation K_{dPAR}; Table 1), stands clearly apart from the other, more turbid and stratified ponds (Fig. S7, lower right plot). In summary, such comparisons between VNIR spectra in surface sediments and selected limnological variables in both surface and bottom waters are promising and should be further explored in forthcoming studies.

Environmental dynamics in thermokarst systems

Most studies in subarctic regions (including northeastern Canada) have considered thermokarst ponds as the final or transitional stage within the thaw/degradation sequence of permafrost mounds, or as an indicator of ancient periglacial forms (Matthews *et al*. 1997; Sollid & Sorbel 1998; Zuidhoff & Kolstrup 2000; Luoto & Seppälä 2003; Payette *et al*. 2004; Vallée & Payette 2007; Calmels *et al*. 2008). Very few studies have extracted the palaeoecological data archived in such aquatic ecosystems (Dallimore *et al*. 2000; Arlen-Pouliot & Bhiry 2005). However, our study shows that thermokarst pond sediments can provide useful and sometimes unexpected palaeoenvironmental insights (e.g. decreasing DOC trends over time) into their natural variability and temporal evolution during their 'life cycle'. Moreover, this study supports the relevance of using VNIR derivative spectral analysis in conjunction with biological proxies (diatoms) to refine palaeolimnological reconstructions in subarctic thermokarst environments.

The recent degradation of permafrost in arctic/subarctic regions is modifying the global carbon pool through multiple feedback mechanisms involving climate, water balance and biogeochemical cycles (Walter *et al*. 2007b; Schuur *et al*. 2008; Laurion *et al*. 2010). With their highly organic waters and catchments, thermokarst ponds and lakes are expected to play a major role in future climate dynamics. However, the controlling processes have yet to be understood and quantified at different temporal and spatial scales. In this regard, multiproxy palaeolimnological studies (such as presented here) that explore the variability and temporal evolution of subarctic thermokarst ponds can help to identify and interpret the biogeochemical processes involved. Among the major factors affecting organic matter properties in subarctic thaw ponds, their developmental stage (age) is likely to control their trophic state and stability (e.g. through microbial community composition, aquatic plant/peat colonization, erosion/suspension of clay particles) (Breton *et al*. 2009). The temporal dynamics of thermokarst ponds and the duration of this aquatic state should therefore have a significant impact on the intensity and direction of future carbon fluxes. More detailed hydrological analyses (e.g. stable isotope analysis of ^{18}O and ^{2}H) are needed to confirm and quantify these relationships.

Conclusions

Despite showing strikingly different limnological conditions, the studied thermokarst ponds revealed comparable palaeolimnological trajectories as recorded in their bottom sediments. Sediment cores consisted of (from bottom to top) (i) postglacial marine silts and clays containing no or very few fossil diatoms (LF), overlain by (ii) organic-rich or peat layers representing ancient summits of permafrost mounds dominated by few aerophilous or bryophilous diatom taxa (TZ), and (iii) finely laminated lacustrine muds deposited since pond inception and showing much higher diatom diversity with truly aquatic taxa (UF). The results of these biostratigraphic analyses demonstrated the major influence of TZ bryophilous substrates (peat layers), which provided aerophilic habitats during pond initial stages and probably controlled diatom community composition.

Moreover, diatom-inferred DOC concentrations in the recent past (i.e. the last 100–150 years) have been decreasing (although only slightly) in all analysed ponds, approaching modern values measured in the field. At the same time, there may have been an increasing trend in pH (related to such a decline in DOC as an organic acid), which cannot be ruled out as a controlling factor on the observed diatom community changes. Thus, the biological and optical diversity of thermokarst ponds, which is related to varying combinations of optically active substances (DOC and TSS), is more likely linked to autogenic and local conditions during and following pond inception (e.g. peat patches and soil stabilization by vegetation development, adsorption of organic matter onto settling clays) rather than to general long-term allogenic/external processes (e.g. precipitation, or alkalinity inherited from regional geology) in the watershed.

Recent landscape changes in permafrost regions and related limnological processes in thermokarst ponds and lakes are of great interest for carbon–climate feedbacks, as carbon greenhouse gas dynamics at high latitudes may be controlled by local factors such as topography, hydrology and vegetation cover. In this regard, the discontinuous peat layers (TZ) identified and described in this study probably represented the major source of organic carbon at early stages of pond evolution, contributing to carbon exchanges between terrestrial and aquatic pools. The studied thermokarst

ponds are similar to many others located along the eastern coast of Hudson Bay, where permafrost features have been rapidly degrading since the early 20th century. These systems apparently played an important role in global biogeochemical cycles in the past and will continue to do so in a rapidly warming world. This aspect, however, needs to be quantified.

Acknowledgements. – We are grateful to C. Dupont, T. Harding, T. Roiha, P.-G. Rossi, A. Rouillard, M. P. Rousseau, D. Sarrazin and S. Watanabe for their assistance in the field; to A.-J. Roy, A.-M. Wagner and E. Saulnier-Talbot for their help in the laboratory; and to M.-A. Fallu, N. Rolland, R. Tremblay and W. F. Vincent for inspiring discussions. R. Crane (Kent State University) conducted the VNIR derivative spectral measurements. We also thank the Cree and Inuit communities of Whapmagoostui and Kuujjuarapik for their support and access to ATV trails; the Centre d'études nordiques (CEN) for logistical support during fieldwork campaigns; and two anonymous reviewers as well as the Editor (Jan A. Piotrowski) for their insightful comments that considerably improved the manuscript. This project was funded through grants from the Fonds de recherche du Québec – Nature et Technologies (FRQNT) awarded to R. Pienitz, P. Francus, I. Laurion and W.F. Vincent; the Natural Sciences and Engineering Research Council of Canada (NSERC) to R. Pienitz and P. Francus; NSERC NCE ArcticNet to I. Laurion; and the Northern Scientific Training Program (NSTP) of Indian and Northern Affairs Canada to F. Bouchard.

References

Agafonov, L., Strunk, H. & Nuber, T. 2004: Thermokarst dynamics in Western Siberia: insights from dendrochronological research. *Palaeogeography, Palaeoclimatology, Palaeoecology 209*, 183–196.

Allard, M. & Seguin, M. K. 1987: Le pergélisol au Québec nordique: bilan et perspectives. *Géographie physique et Quaternaire 41*, 141–152.

Allard, M. & Tremblay, G. 1983: La dynamique littorale des îles Manitounuk durant l'Holocène. *Zeitschrift für Geomorphologie, Supplementbände 47*, 61–95.

Anderson, N. J. 1990: Variability of diatom concentrations and accumulation rates in sediments of a small lake basin. *Limnology and Oceanography 35*, 497–508.

Arlen-Pouliot, Y. & Bhiry, N. 2005: Palaeoecology of a palsa and a filled thermokarst pond in a permafrost peatland, subarctic Quebec, Canada. *The Holocene 15*, 408–419.

Barber, D. C., Dyke, A. S., Hillaire-Marcel, C., Jennings, A. E., Andrews, J. T., Kerwin, M. W., Bilodeau, G., McNeely, R., Southon, J., Morehead, M. D. & Gagnon, J.-M. 1999: Forcing of the cold event of 8,200 years ago by catastrophic drainage of Laurentide lakes. *Nature 400*, 344–348.

Battarbee, R., Jones, V., Flower, R., Cameron, N., Bennion, H., Carvalho, L. & Juggins, S. 2002: Diatoms. *In* Smol, J., Birks, J., Last, W., Bradley, R. & Alverson, K. (eds): *Tracking Environmental Change Using Lake Sediments, Vol. 3: Terrestrial, Algal, and Siliceous Indicators*, 155–202. Kluwer Academic Publishers, Dordrecht.

Beilman, D. W., Vitt, D. H. & Halsey, L. A. 2001: Localized permafrost peatlands in Western Canada: definition, distributions, and degradation. *Arctic Antarctic and Alpine Research 33*, 70–77.

Bhiry, N. & Robert, E. C. 2006: Reconstruction of changes in vegetation and trophic conditions of a palsa in a permafrost peatland, subarctic Québec, Canada. *Ecoscience 13*, 56–65.

Bhiry, N., Delwaide, A., Allard, M., Begin, Y., Filion, L., Lavoie, M., Nozais, C., Payette, S., Pienitz, R., Saulnier-Talbot, E. & Vincent, W. F. 2011: Environmental change in the Great Whale River region, Hudson Bay: five decades of multidisciplinary research by Centre d'etudes nordiques (CEN). *Ecoscience 18*, 182–203.

Bouchard, F., Francus, P., Pienitz, R. & Laurion, I. 2011: Sedimentology and geochemistry of thermokarst ponds in discontinuous permafrost, subarctic Quebec, Canada. *Journal of Geophysical Research-Biogeosciences 116*, G00M04, doi: 10.1029/2011JG001675.

Breton, J., Vallières, C. & Laurion, I. 2009: Limnological properties of permafrost thaw ponds in northeastern Canada. *Canadian Journal of Fisheries and Aquatic Sciences 66*, 1635–1648.

Brown, J., Ferrians, O. J., Heginbottom, J. A. & Melnikov, E. S. 1998: *Circum-Arctic Map of Permafrost and Ground-Ice Conditions*. Revised Feb. 2001. National Snow and Ice Data Center/World Data Center for Glaciology, Boulder, CO.

Calmels, F. & Allard, M. 2008: Segregated ice structures in various heaved permafrost landforms through CT scan. *Earth Surface Processes and Landforms 33*, 209–225.

Calmels, F., Allard, M. & Delisle, G. 2008: Development and decay of a lithalsa in Northern Quebec: a geomorphological history. *Geomorphology 97*, 287–299.

Christensen, T. R., Johansson, T., Ökerman, H. J., Mastepanov, M., Malmer, N., Friborg, T., Crill, P. & Svensson, B. H. 2004: Thawing sub-arctic permafrost: effects on vegetation and methane emissions. *Geophysical Research Letters 31*, L04501, doi: 10.1029/2003GL018680.

Croudace, I. W., Rindby, A. & Rothwell, R. G. 2006: ITRAX: description and evaluation of a new multi-function X-ray core scanner. *In* Rothwell, R. G. 2006 (ed.): *New Techniques in Sediment Core Analysis*, 51–63. *Geological Society, London, Special Publication 267*.

Dallimore, A., Schröder-Adams, C. J. & Dallimore, S. R. 2000: Holocene environmental history of thermokarst lakes on Richards Island, Northwest Territories, Canada: theocamoebians as paleolimnological indicators. *Journal of Paleolimnology 23*, 261–283.

Debret, M., Sebag, D., Desmet, M., Balsam, W., Copard, Y., Mourier, B., Susperrigui, A. S., Arnaud, F., Bentaleb, I., Chapron, E., Lallier-Vergès, E. & Winiarski, T. 2011: Spectrocolorimetric interpretation of sedimentary dynamics: the new 'Q7/4 diagram'. *Earth-Science Reviews 109*, 1–19.

Dyke, A. S. & Prest, V. K. 1987: Late Wisconsinan and Holocene history of the Laurentide Ice Sheet. *Géographie physique et Quaternaire 41*, 237–263.

Ellis, C. J., Rochefort, L., Gauthier, G. & Pienitz, R. 2008: Paleoecological evidence for transitions between contrasting landforms in a polygon-patterned high Arctic wetland. *Arctic, Antarctic, and Alpine Research 40*, 624–637.

Environment Canada 2010: *Canadian climate normals or averages 1971–2000*. Available at: http://climate.weatheroffice.gc.ca/climate_normals/index_e.html (accessed 14.11.2012).

Fallu, M. A. & Pienitz, R. 1999: Lacustrine diatoms in the Hudson Bay and James Bay area of Quebec – reconstruction of dissolved organic carbon concentrations. *Ecoscience 6*, 603–620.

Fallu, M. A., Allaire, N. & Pienitz, R. 2000: *Freshwater Diatoms from Northern Québec and Labrador (Canada): Species-Environment Relationships in Lakes of Boreal Forest, Forest-Tundra and Tundra Regions*. 200 pp. J. Cramer, Berlin.

Grenier, M., Campeau, S., Lavoie, I., Park, Y. S. & Lek, S. 2006: Diatom reference communities in Quebec (Canada) streams based on Kohonen self-organizing maps and multivariate analyses. *Canadian Journal of Fisheries and Aquatic Sciences 63*, 2087–2106.

Hill, M. O. & Gauch, H. G. 1980: Detrended correspondence analysis: an improved ordination technique. *Vegetatio 42*, 47–58.

Hillaire-Marcel, C. 1976: La déglaciation et le relèvement isostatique sur la côte est de la baie d'Hudson. *Cahiers de géographie du Québec 20*, 185–220.

Hillaire-Marcel, C., Occhietti, S. & Vincent, J.-S. 1981: Sakami moraine, Quebec: a 500-km-long moraine without climatic control. *Geology 9*, 210–214.

Jorgenson, M. T., Shur, Y. L. & Pullman, E. R. 2006: Abrupt increase in permafrost degradation in Arctic Alaska. *Geophysical Research Letters 33*, L02503, doi: 10.1029/2005gl024960.

Juggins, S. 2007: *C2 Version 1.5: Software for Ecological and Palaeoecological Data Analysis and Visualisation*. University of Newcastle, Newcastle upon Tyne.

Konrad, J. M. & Seto, J. T. C. 1994: Frost heave characteristics of undisturbed sensitive Champlain Sea clay. *Canadian Geotechnical Journal 31*, 285–298.

Krammer, K. 2000: The genus Pinnularia. *In* Lange-Bertalot, H. (ed.): *Diatoms of Europe. Diatoms of the European Inland Waters and Comparable Habitats*, Vol. *1*, 703pp. A.R.G. Gantner Verlag K.G., Ruggell.

Krammer, K. 2002: Cymbella. *In* Lange-Bertalot, H. (ed.): *Diatoms of Europe. Diatoms of the European Inland Waters and Comparable Habitats*, Vol. *3*, 584pp. A.R.G. Gantner Verlag K.G., Ruggell.

Krammer, K. & Lange-Bertalot, H. 1986: Bacillariophyceae 1. Teil: Naviculaceae. *In* Ettl, H., Gerloff, J., Heynig, H. & Mollenhauer, D. (eds): *Süßwasserflora von Mitteleuropa, Band 2/1*, 876pp. Gustav Fischer Verlag, Stuttgart.

Krammer, K. & Lange-Bertalot, H. 1988: Bacillariophyceae 2. Teil: Bacillariaceae, Epithemiaceae, Surirellaceae. *In* Ettl, H., Gerloff, J., Heynig, H. & Mollenhauer, D. (eds): *Süßwasserflora von Mitteleuropa, Band 2/2*, 596pp. Gustav Fischer Verlag, Stuttgart.

Krammer, K. & Lange-Bertalot, H. 1991a: Bacillariophyceae 3. Teil: Centrales, Fragilariaceae, Eunotiaceae. *In* Ettl, H., Gerloff, J., Heynig, H. & Mollenhauer, D. (eds): *Süßwasserflora von Mitteleuropa, Band 2/3*, 576pp. Gustav Fischer Verlag, Stuttgart.

Krammer, K. & Lange-Bertalot, H. 1991b: Bacillariophyceae 4. Teil: Achnanthaceae, Kritische Ergänzungen zu Navicula (Lineolatae) und Gomphonema Gesamtliteraturverzeichnis Teil 1-4. *In* Ettl, H., Gerloff, J., Heynig, H. & Mollenhauer, D. (eds): *Süßwasserflora von Mitteleuropa, Band 2/4*, 436pp. Gustav Fischer Verlag, Stuttgart.

Lajeunesse, P. 2008: Early Holocene deglaciation of the eastern coast of Hudson Bay. *Geomorphology 99*, 341–352, doi: 10.1016/j.geomorph.2007.11.012.

Lajeunesse, P. & St-Onge, G. 2008: The subglacial origin of the lake Agassiz-Ojibway final outburst flood. *Nature Geoscience 1*, 184–188.

Laurion, I., Vincent, W. F., MacIntyre, S., Retamal, L., Dupont, C., Francus, P. & Pienitz, R. 2010: Variability in greenhouse gas emissions from permafrost thaw ponds. *Limnology and Oceanography 55*, 115–133.

Lavoie, I., Hamilton, P. B., Campeau, S., Grenier, M. & Dillon, P. J. 2008: *Guide d'identification des diatomées des rivières de l'Est du Canada*. 241 pp. Presses de l'Université du Québec, Québec.

Luoto, M. & Seppälä, M. 2003: Thermokarst ponds as indicators of the former distribution of palsas in Finnish Lapland. *Permafrost and Periglacial Processes 14*, 19–27.

Matthews, J. A., Dahl, S. O., Berrisford, M. S. & Nesje, A. 1997: Cyclic development and thermokarstic degradation of palsas in the mid-alpine zone at Leirpullan, Dovrefjell, southern Norway. *Permafrost and Periglacial Processes 8*, 107–122.

Moser, K. A., Korhola, A., Wekcström, J., Blom, T., Pienitz, R., Smol, J. P., Douglas, M. S. V. & Hay, M. B. 2000: Paleohydrology inferred from diatoms in northern latitude regions. *Journal of Paleolimnology 24*, 93–107.

Ortiz, J. D. 2011: Application of Visible/near Infrared derivative spectroscopy to Arctic paleoceanography. *IOP Conference Series: Earth and Environmental Science 14*, 012011, pp. 1–13, doi: 10.1088/1755-1315/14/1/012011.

Ortiz, J. D., O'Connell, S. B., DelViscio, J., Dean, W., Carriquiry, J. D., Marchitto, T., Zheng, Y. & van Geen, A. 2004: Enhanced marine productivity off western North America during warm climate intervals of the past 52 ky. *Geology 32*, 521–524.

Ortiz, J. D., Polyak, L., Grebmeier, J. M., Darby, D., Eberl, D. D., Naidu, S. & Nof, D. 2009: Provenance of Holocene sediment on the Chukchi-Alaskan margin based on combined diffuse spectral reflectance and quantitative X-Ray Diffraction analysis. *Global and Planetary Change 68*, 71–84.

Osterkamp, T. E. 2007: Characteristics of the recent warming of permafrost in Alaska. *Journal of Geophysical Research-Earth Surface 112*, F02S02, doi: 10.1029/2006jf000578.

Payette, S., Delwaide, A., Caccianiga, M. & Beauchemin, M. 2004: Accelerated thawing of subarctic peatland permafrost over the last 50 years. *Geophysical Research Letters 31*, L18208, doi: 10.1029/2004GL020358.

Pienitz, R. 2001: Analyse des microrestes végétaux: diatomées. *In* Payette, S. & Rochefort, L. (eds): *Écologie des tourbières du Québec-Labrador*, 311–326. Les Presses de l'Université Laval, Québec.

Pienitz, R. & Vincent, W. F. 2000: Effect of climate change relative to ozone depletion on UV exposure in subarctic lakes. *Nature 404*, 484–487.

Pienitz, R., Doran, P. T. & Lamoureux, S. F. 2008: Origin and geomorphology of lakes in the polar regions. *In* Vincent, W. & Laybourn-Parry, J. (eds): *Polar Lakes and Rivers: Limnology of Arctic and Antarctic Aquatic Ecosystems*, 25–41. Oxford University Press, Oxford.

Pienitz, R., Smol, J. P. & Birks, H. J. B. 1995: Assessment of freshwater diatoms as quantitative indicators of past climatic change in the Yukon and Northwest Territories, Canada. *Journal of Paleolimnology 13*, 21–49.

Pienitz, R., Smol, J. P. & MacDonald, G. M. 1999: Paleolimnological reconstruction of Holocene climatic trends from two boreal treeline lakes, Northwest Territories, Canada. *Arctic Antarctic and Alpine Research 31*, 82–93.

Pissart, A. 2002: Palsas, lithalsas and remnants of these periglacial mounds. A progress report. *Progress in Physical Geography 26*, 605–621.

Ponader, K., Pienitz, R., Vincent, W. F. & Gajewski, K. 2002: Limnological conditions in a subarctic lake (northern Québec, Canada) during the late Holocene: analyses based on fossil diatoms. *Journal of Paleolimnology 27*, 353–366.

Saulnier-Talbot, E. & Pienitz, R. 2001: Postglacial isolation of a coastal basin near Kuujjuaraapik-Whapmagoostui, Hudsonie: a diatom biostratigraphical investigation. *Géographie physique et Quaternaire 55*, 63–74.

Saulnier-Talbot, E., Pienitz, R. & Vincent, W. F. 2003: Holocene lake succession and palaeo-optics of a Subarctic lake, northern Quebec, Canada. *The Holocene 13*, 517–526.

Schuur, E. A. G., Bockheim, J. G., Canadell, J. G., Euskirchen, E., Field, C. B., Goryachkin, S. V., Hagemann, S., Kuhry, P., Lafleur, P. M., Lee, H., Mazhitova, G., Nelson, F. E., Rinke, A., Romanovsky, V. E., Shiklomanov, N., Tarnocai, C., Venevsky, S., Vogel, J. G. & Zimov, S. A. 2008: Vulnerability of permafrost carbon to climate change: implications for the global carbon cycle. *BioScience 58*, 701–714.

Schuur, E. A. G., Vogel, J. G., Crummer, K. G., Lee, H., Sickman, J. O. & Osterkamp, T. E. 2009: The effect of permafrost thaw on old carbon release and net carbon exchange from tundra. *Nature 459*, 556–559.

Sollid, J. L. & Sorbel, L. 1998: Palsa bogs as a climate indicator – Examples from Dovrefjell, southern Norway. *Ambio 27*, 287–291.

Stevenson, A. C., Juggins, S., Birks, H. J. B., Anderson, D. S., Anderson, N. J., Battarbee, R. W., Berge, F., Davis, R. B., Flower, R. J., Haworth, E. Y., Jones, V. J., Kingston, J. C., Kreiser, A. M., Line, J. M., Munro, M. A. R. & Renberg, I. 1991: *The Surface Waters Acidification Project Palaeolimnology Programme: Modern Diatom/Lake-Water Chemistry Data-Set*. 86 pp. ENSIS Publishing, London.

Takakai, F., Desyatkin, A. R., Lopez, C. M. L., Fedorov, A. N., Desyatkin, R. V. & Hatano, R. 2008: CH4 and N2O emissions from a forest-alas ecosystem in the permafrost taiga forest region, eastern Siberia, Russia. *Journal of Geophysical Research-Biogeosciences 113*, G02002, doi: 10.1029/2007jg000521.

Tarnocai, C., Canadell, J. G., Schuur, E. A. G., Kuhry, P., Mazhitova, G. & Zimov, S. 2009: Soil organic carbon pools in the northern circumpolar permafrost region. *Global Biogeochemical Cycles 23*, GB2023, doi: 10.1029/2008GB003327.

ter Braak, C. J. F. & Šmilauer, P. 2002: *CANOCO Reference Manual and CanoDraw for Windows User's Guide: Software for Canonical Community Ordination (Version 4.5)*. 500 pp. Microcomputer Power, Ithaca, NY.

Tietjen, T., Vähätalo, A. V. & Wetzel, R. G. 2005: Effects of clay mineral turbidity on dissolved organic carbon and bacterial production. *Aquatic Sciences – Research Across Boundaries 67*, 51–60.

Turner, K. W., Wolfe, B. B. & Edwards, T. W. D. 2010: Characterizing the role of hydrological processes on lake water balances in the Old Crow Flats, Yukon Territory, Canada, using water isotope tracers. *Journal of Hydrology 386*, 103–117.

Vallée, S. & Payette, S. 2007: Collapse of permafrost mounds along a subarctic river over the last 100 years (northern Quebec). *Geomorphology 90*, 162–170.

van Huissteden, J., Berrittella, C., Parmentier, F. J. W., Mi, Y., Maximov, T. C. & Dolman, A. J. 2011: Methane emissions from permafrost thaw lakes limited by lake drainage. *Nature Climate Change 1*, 119–123.

Veillette, J. J. 1994: Evolution and paleohydrology of glacial Lakes Barlow and Ojibway. *Quaternary Science Reviews 13*, 945–971.

von Gunten, L., Grosjean, M., Rein, B., Urrutia, R. & Appleby, P. 2009: A quantitative high-resolution summer temperature reconstruction based on sedimentary pigments from Laguna Aculeo, central Chile, back to AD 850. *Holocene 19*, 873–881.

Walter, K. M., Edwards, M. E., Grosse, G., Zimov, S. A. & Chapin, F. S. 2007a: Thermokarst lakes as a source of atmospheric CH4 during the last deglaciation. *Science 318*, 633–636.

Walter, K. M., Smith, L. C. & Chapin, F. S. 2007b: Methane bubbling from northern lakes: present and future contributions to the global methane budget. *Philosophical Transactions of the Royal Society A -Mathematical Physical and Engineering Sciences 365*, 1657–1676.

Walter, K. M., Zimov, S. A., Chanton, J. P., Verbyla, D. & Chapin, F. S. 2006: Methane bubbling from Siberian thaw lakes as a positive feedback to climate warming. *Nature 443*, 71–75.

Watanabe, S., Laurion, I., Pienitz, R., Chokmani, K. & Vincent, W. F. 2011: Optical diversity of thaw ponds in discontinuous permafrost: a model system for water color analysis. *Journal of Geophysical Research-Biogeosciences 116*, G02003, doi: 10.1029/2010JG001380.

Weckström, J., Korhola, A. & Blom, T. 1997: Diatoms as quantitative indicators of pH and water temperature in subarctic Fennoscandian lakes. *Hydrobiologia 347*, 171–184.

Wolfe, A. P. 1997: On diatom concentrations in lake sediments: results from an inter-laboratory comparison and other tests performed on a uniform sample. *Journal of Paleolimnology 18*, 261–268.

Yurco, L. N., Ortiz, J. D., Polyak, L., Darby, D. A. & Crawford, K. A. 2010: Clay mineral cycles identified by diffuse spectral reflectance in Quaternary sediments from the Northwind Ridge: implications for glacial-interglacial sedimentation patterns in the Arctic Ocean. *Polar Research 29*, 176–197.

Zimov, S. A., Schuur, E. A. G. & Chapin, F. S. 2006: Permafrost and the global carbon budget. *Science 312*, 1612–1613.

Zuidhoff, F. S. & Kolstrup, E. 2000: Changes in palsa distribution in relation to climate change in Laivadalen, northern Sweden, especially 1960–1997. *Permafrost and Periglacial Processes 11*, 55–69.

Supporting Information

Additional Supporting Information may be found in the online version of this article:

Fig. S1. Diatom abundance diagram (expressed as relative frequencies) for core K1 (brown pond). UF = upper facies (lacustrine); LF = lower facies (marine); TZ = transition zone (peat/organic) between UF and LF.

Fig. S2. Diatom abundance diagram (expressed as relative frequencies) for core K2 (black pond). UF = upper facies (lacustrine); LF = lower facies (marine); TZ = transition zone (peat/organic) between UF and LF.

Fig. S3. Diatom abundance diagram (expressed as relative frequencies) for core K6 (green pond). UF = upper facies (lacustrine); LF = lower facies (marine); TZ = transition zone (peat/organic) between UF and LF.

Fig. S4. Diatom abundance diagram (expressed as relative frequencies) for core K12 (black pond). UF = upper facies (lacustrine); LF = lower facies (marine); TZ = transition zone (peat/organic) between UF and LF. Chronology (^{210}Pb) is not available for this particular core.

Fig. S5. Diatom abundance diagram (expressed as relative frequencies) for core K16 (beige pond). UF = upper facies (lacustrine); LF = lower facies (marine); TZ = transition zone (peat/organic) between UF and LF.

Fig. S6. Diatom abundance diagram (expressed as relative frequencies) for core K20 (beige pond). UF = upper facies (lacustrine); LF = lower facies (marine); TZ = transition zone (peat/organic) between UF and LF.

Fig. S7. Correlation plots between varimax-rotated components (VPCA) in surface sediments (x-axis) and selected limnological properties in pond water (y-axis). More correlations are presented in Table S6.

Table S1. Complete list of identified diatom taxa, including species codes, species names (as mentioned in Fallu *et al.* (2000) and other used floras) and species synonyms. See Materials and methods for details.

Table S2. Detailed diatom and microsphere counts for each analysed pond (1 worksheet/pond=6 worksheets).

Table S3. Detailed results (sample scores) of the detrended correspondence analysis (DCA) of analysed ponds, including eigenvalues (λ), gradient lengths and cumulative percentage variance of species data for the first four DCA axes.

Table S4. Eigenvalues and percentage variance for the leading components extracted by variable-based principal component analysis (PCA), before and after varimax rotation.

Table S5. Significant correlations ($p<0.01$) between VPCA components of VNIR reflectance data, diatom taxa and major geochemical elements (XRF).

Table S6. Principal correlations ($r>0.80$) between varimax-rotated components (VPCA) in surface sediments, selected diatom data in surface sediments and limnological properties in pond water.